

LARGE EDDY SIMULATION (LES)

Lars Davidson, www.tfd.chalmers.se/~lada
Chalmers University of Technology
Gothenburg, Sweden

THREE-DAY CFD COURSE AT CHALMERS

- ▶ This lecture is a condensed version of the course
 - **Unsteady Simulations** for Industrial Flows: LES, DES, hybrid LES-RANS and URANS
 - **5-7 November** 2012 at Chalmers, Gothenburg, Sweden
 - Max **16** participants
 - 50% lectures and **50% workshops** in front of a PC
 - For info, see <http://www.tfd.chalmers.se/~lada/cfdkurs/cfdkurs.html>

LECTURE NOTES

- The slides are partly based on the course material at [\(click here\)](#)

`http://www.tfd.chalmers.se/~lada/
comp_turb_model/lecture_notes.html`

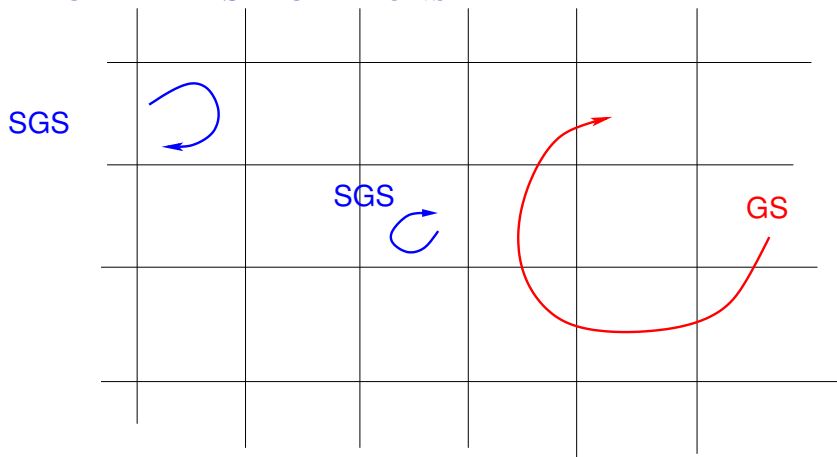
- This course is part of the MSc programme **Applied Mechanics** at Chalmers. For Fluid courses, [click here](#)

`http://www.tfd.chalmers.se/~lada/
msc/msc-programme.html`

- The MSc programme is presented [here](#)

`http://www.chalmers.se/en/education/programmes/mast`

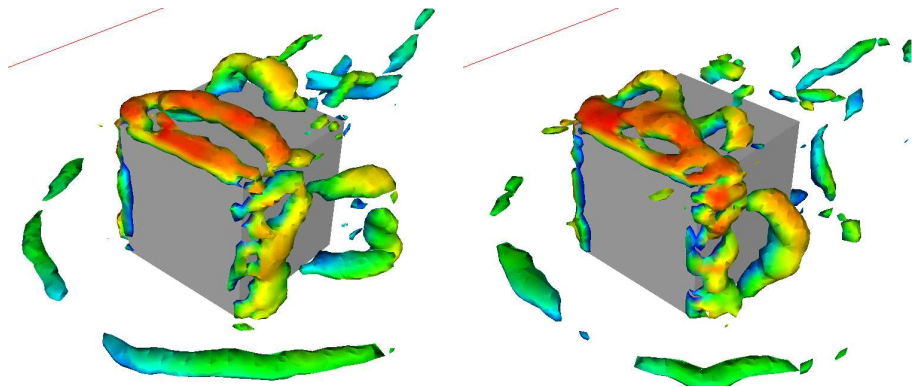
LARGE EDDY SIMULATIONS



- In LES, large (**G**rid) **S**cales (**GS**) are resolved and the small (**S**ub-**G**rid) **S**cales (**SGS**) are modelled.
- **LES** is suitable for bluff body flows where the flow is governed by large turbulent scales

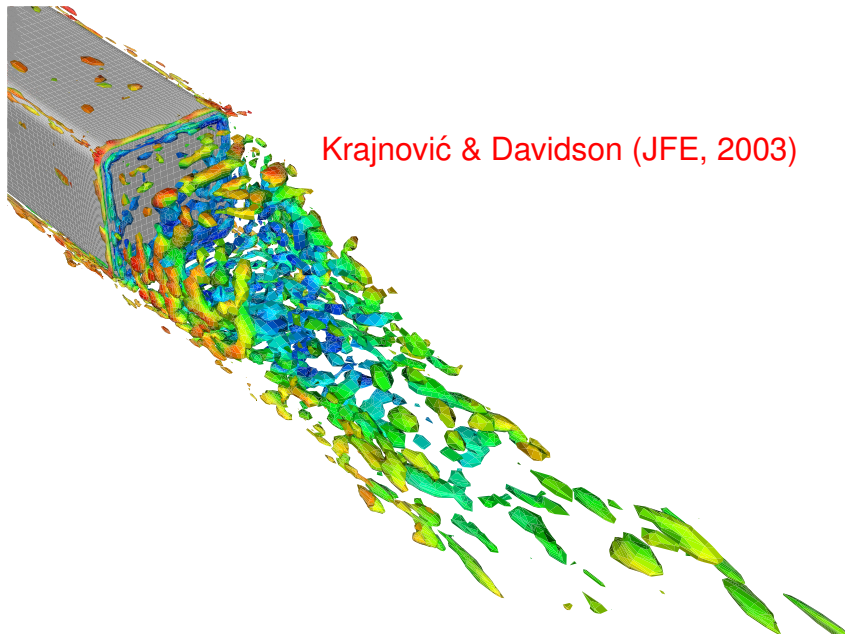
BLUFF-BODY FLOW: SURFACE-MOUNTED CUBE[14]

Krajnović & Davidson (AIAA J., 2002)



Snapshots of large turbulent scales illustrated by $Q = -\frac{\partial \bar{u}_i}{\partial x_j} \frac{\partial \bar{u}_j}{\partial x_i}$

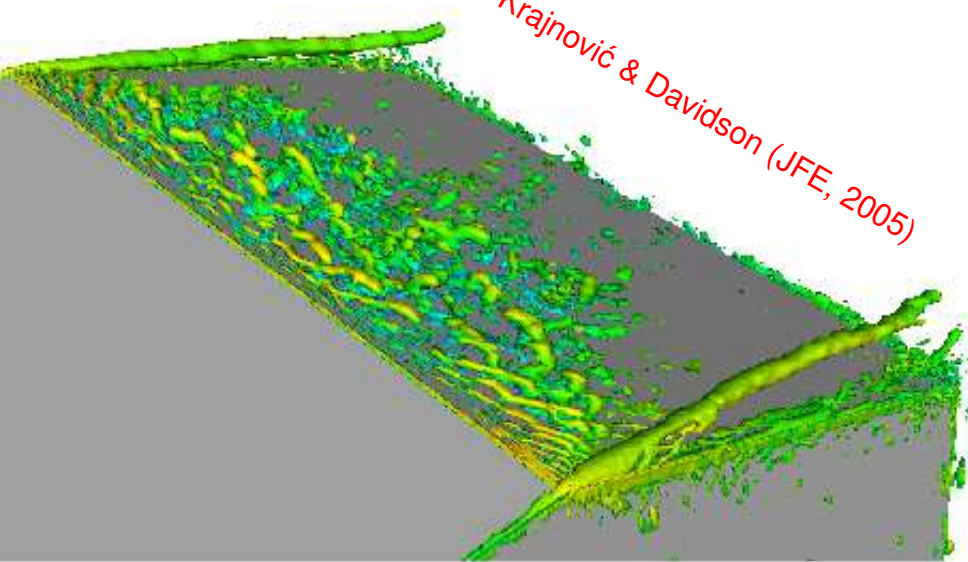
BLUFF-BODY FLOW: FLOW AROUND A BUS[15]



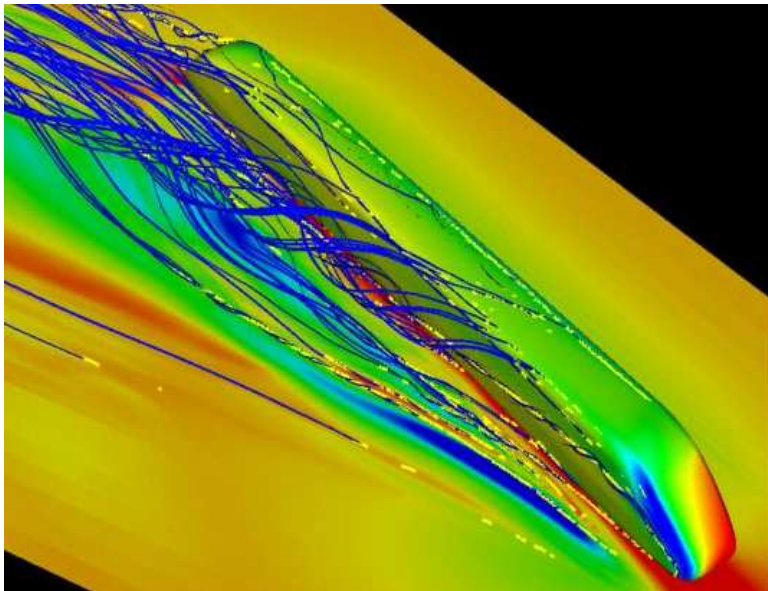
Krajnović & Davidson (JFE, 2003)

BLUFF-BODY FLOW: FLOW AROUND A CAR[16]

Krajnović & Davidson (JFE, 2005)

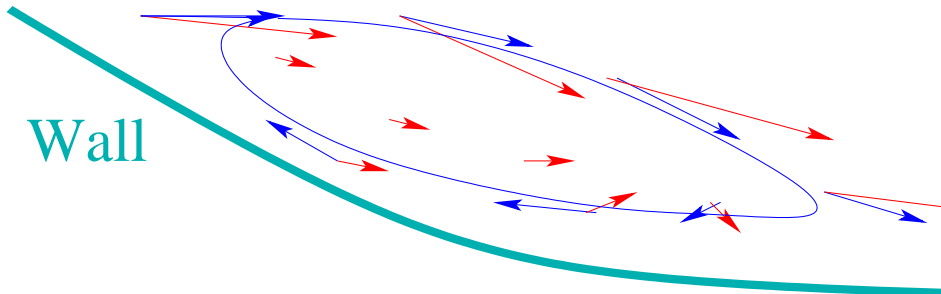


BLUFF-BODY FLOW: FLOW AROUND A TRAIN[12]



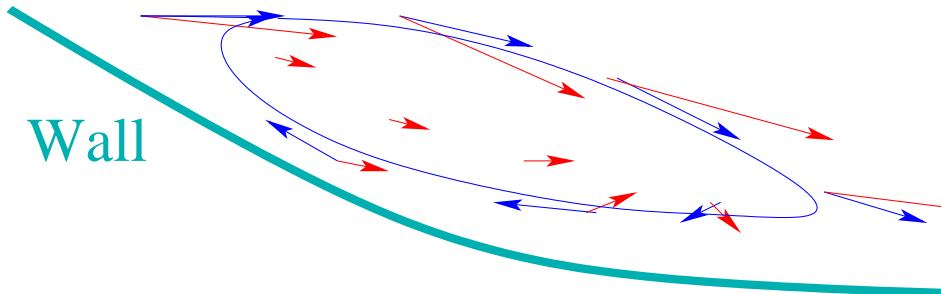
Hemida & Krajnović, 2006

SEPARATING FLOWS



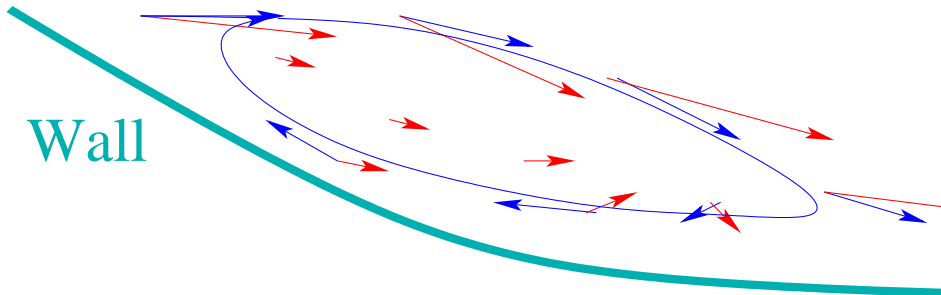
- TIME-AVERAGED flow and INSTANTANEOUS flow

SEPARATING FLOWS



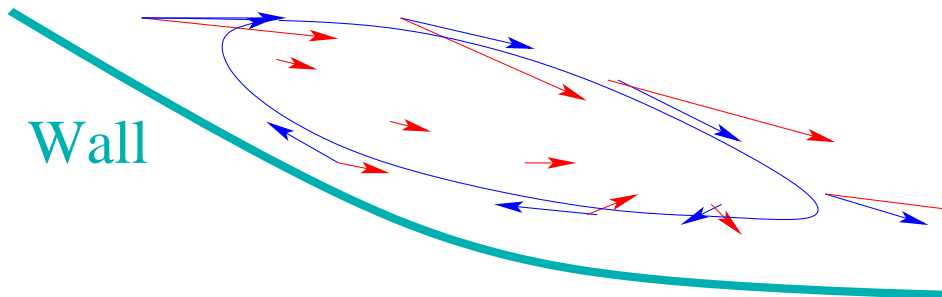
- **TIME-AVERAGED** flow and **INSTANTANEOUS** flow
- In average there is backflow (negative velocities). **Instantaneous**, the negative velocities are often positive.

SEPARATING FLOWS



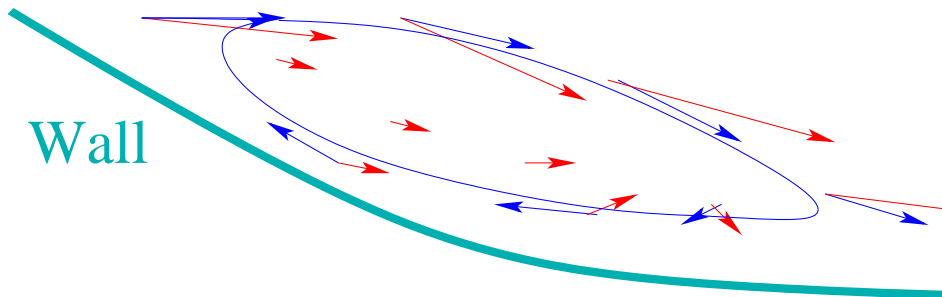
- **TIME-AVERAGED** flow and **INSTANTANEOUS** flow
- In average there is backflow (negative velocities). **Instantaneous**, the negative velocities are often positive.
- How easy is it to model fluctuations that are as large as the mean flow?

SEPARATING FLOWS



- **TIME-AVERAGED** flow and **INSTANTANEOUS** flow
- In average there is backflow (negative velocities). **Instantaneous**, the negative velocities are often positive.
- How easy is it to model fluctuations that are as large as the mean flow?
- Is it reasonable to require a turbulence model to fix this?

SEPARATING FLOWS



- **TIME-AVERAGED** flow and **INSTANTANEOUS** flow
- In average there is backflow (negative velocities). **Instantaneous**, the negative velocities are often positive.
- How easy is it to model fluctuations that are as large as the mean flow?
- Is it reasonable to require a turbulence model to fix this?
- Isn't it better to **RESOLVE** the large fluctuations?

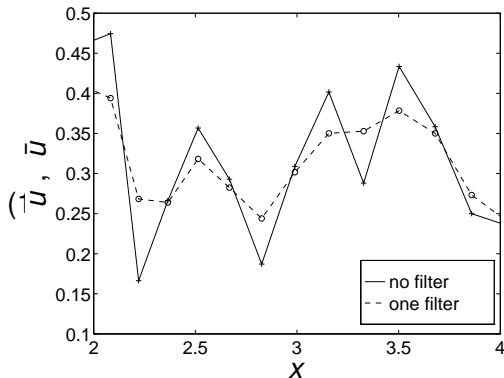
TIME AVERAGING AND FILTERING

RANS: time average. This is called Reynolds time averaging:

$$\langle \Phi \rangle = \frac{1}{2T} \int_{-T}^T \Phi(t) dt, \quad \Phi = \langle \Phi \rangle + \Phi'$$

In LES we filter (volume average) the equations. In 1D we get:

$$\bar{\Phi}(x, t) = \frac{1}{\Delta x} \int_{x-0.5\Delta x}^{x+0.5\Delta x} \Phi(\xi, t) d\xi$$
$$\Phi = \bar{\Phi} + \Phi''$$



EQUATIONS

- The filtering is defined by the discretization (**nothing** is done)
- The filtered Navier-Stokes (N-S) eqns, i.e. the LES eqns, read

$$\frac{\partial \bar{u}_i}{\partial t} + \frac{\partial}{\partial x_j} (\bar{u}_i \bar{u}_j) = -\frac{1}{\rho} \frac{\partial \bar{p}}{\partial x_i} + \nu \frac{\partial^2 \bar{u}_i}{\partial x_j \partial x_j} - \frac{\partial \tau_{ij}}{\partial x_j}, \quad \frac{\partial \bar{u}_i}{\partial x_i} = 0 \quad (2)$$

where the subgrid stresses are given by

$$\tau_{ij} = \overline{u_i u_j} - \bar{u}_i \bar{u}_j$$

Contrary to Reynolds time averaging where $\langle u_i' \rangle = 0$, we have here

$$\overline{u_i'} \neq 0 \quad \bar{\bar{u}}_i \neq \bar{u}_i$$

FILTERING: HOW IS EQ. 2 OBTAINED?

- The N-S eqns are filtered (=discretized) using Eq. 1
- The pressure gradient term, for example, reads

$$\overline{\frac{\partial p}{\partial x_i}} = \frac{1}{V} \int_V \frac{\partial p}{\partial x_i} dV$$

- Now we want to move the derivative out of the integral. It is allowed if V is constant.
- The filtering volume, V =grid cell which is **not** constant
- Fortunately, the error is proportional to V^2 , i.e. it is 2nd-order error

$$\overline{\frac{\partial p}{\partial x_i}} = \frac{\partial}{\partial x_i} \left(\frac{1}{V} \int_V p dV \right) + \mathcal{O}(V^2) = \frac{\partial}{\partial x_i}(\bar{p}) + \mathcal{O}(V^2)$$

All linear terms are treated in the same way.

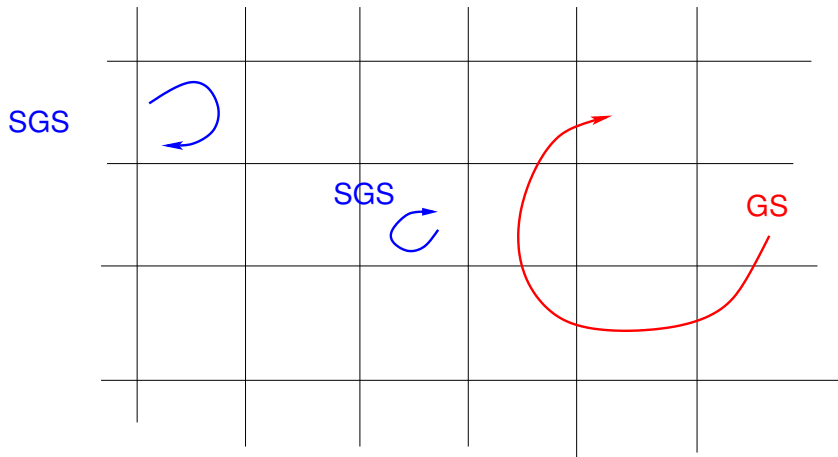
NON-LINEAR TERM

- First we filter the term and move the derivative out of the integral

$$\overline{\frac{\partial u_i u_j}{\partial x_j}} = \frac{\partial}{\partial x_j} \left(\frac{1}{V} \int_V u_i u_j dV \right) + \mathcal{O}(V^2) = \frac{\partial}{\partial x_j} (\overline{u_i u_j}) + \mathcal{O}(V^2)$$

- We have $\frac{\partial}{\partial x_j} \overline{u_i u_j}$; we want $\frac{\partial}{\partial x_j} \bar{u}_i \bar{u}_j$
- Let's add what we want (on both LHS and RHS) and subtract what we don't want
- This is how we end up with the convective term and the SGS term in Eq. 2, i.e. $-\frac{\partial \tau_{ij}}{\partial x_j} = -\frac{\partial}{\partial x_j} (\overline{u_i u_j} - \bar{u}_i \bar{u}_j)$

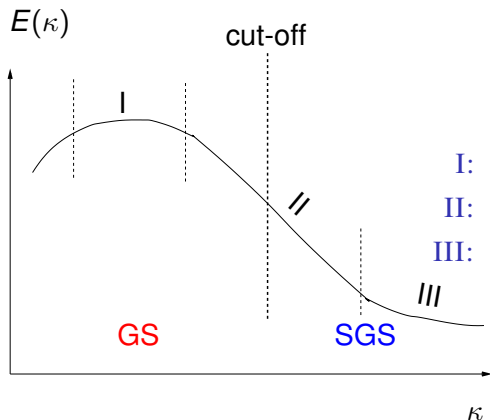
LARGE EDDY SIMULATIONS



- Large scales (**GS**) are resolved; small scales (**SGS**) are modelled.

ENERGY SPECTRUM

The limit (cut-off) between **GS** and **SGS** is supposed to take place in the inertial subrange (II)



I: large scales

II: inertial subrange, $-5/3$ -range

III: dissipation subrange

SUBGRID MODEL

- We need a subgrid model for the SGS turbulent scales
- The simplest model is the Smagorinsky model [23]:

$$\tau_{ij} - \frac{1}{3}\delta_{ij}\tau_{kk} = -2\nu_{sgs}\bar{s}_{ij}$$
$$\nu_{sgs} = (C_S\Delta)^2 \sqrt{2\bar{s}_{ij}\bar{s}_{ij}} \equiv (C_S\Delta)^2 |\bar{s}| \quad (3)$$
$$\bar{s}_{ij} = \frac{1}{2} \left(\frac{\partial \bar{u}_i}{\partial x_j} + \frac{\partial \bar{u}_j}{\partial x_i} \right), \quad \Delta = (\Delta V_{IJK})^{1/3}$$

- A damping function f_μ is added to ensure that $\nu_{sgs} \Rightarrow 0$ as $y \Rightarrow 0$
$$f_\mu = 1 - \exp(-y^+/26)$$
- A more convenient way to dampen the SGS viscosity near the wall is

$$\Delta = \min \left\{ (\Delta V_{IJK})^{1/3}, \kappa y \right\}$$

where y is the distance to the nearest wall.

SMAGORINSKY MODEL VS. MIXING-LENGTH MODEL

- The eddy viscosity in the mixing length model reads in boundary-layer flow [13, 22]

$$\nu_t = \ell^2 \left| \frac{\partial U}{\partial y} \right|.$$

- Generalized to three dimensions, we have

$$\nu_t = \ell^2 \left[\left(\frac{\partial U_i}{\partial x_j} + \frac{\partial U_j}{\partial x_i} \right) \frac{\partial U_i}{\partial x_j} \right]^{1/2} = \ell^2 (2S_{ij}S_{ij})^{1/2} \equiv \ell^2 |S|.$$

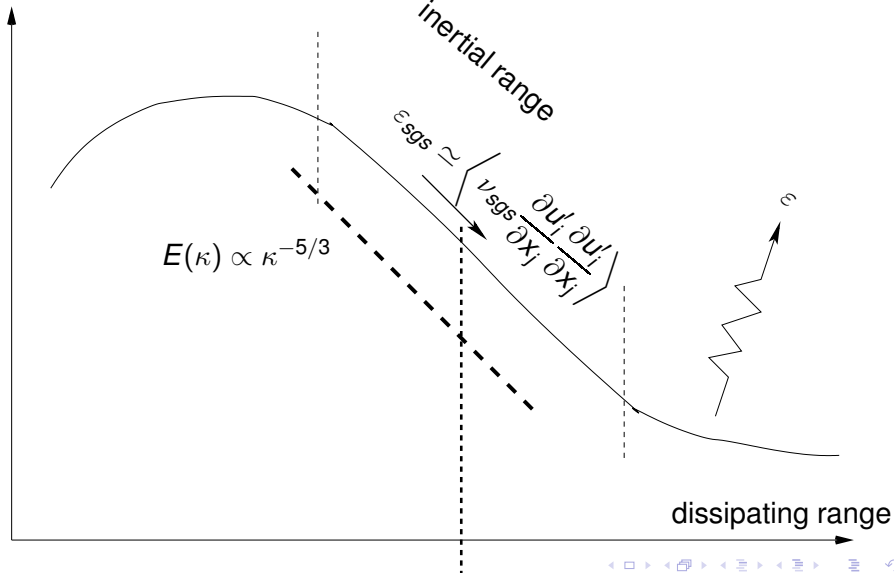
- In the Smagorinsky model the SGS length scale $\ell = C_S \Delta$ i.e.

$$\nu_{sgs} = (C_S \Delta)^2 |\bar{s}|$$

which is the same as Eq. 3

ENERGY PATH

$E(\kappa)$



LES vs. RANS

LES can handle many flows which RANS (Reynolds Averaged Navier Stokes) cannot; the reason is that in LES large, turbulent scales are resolved. Examples are:

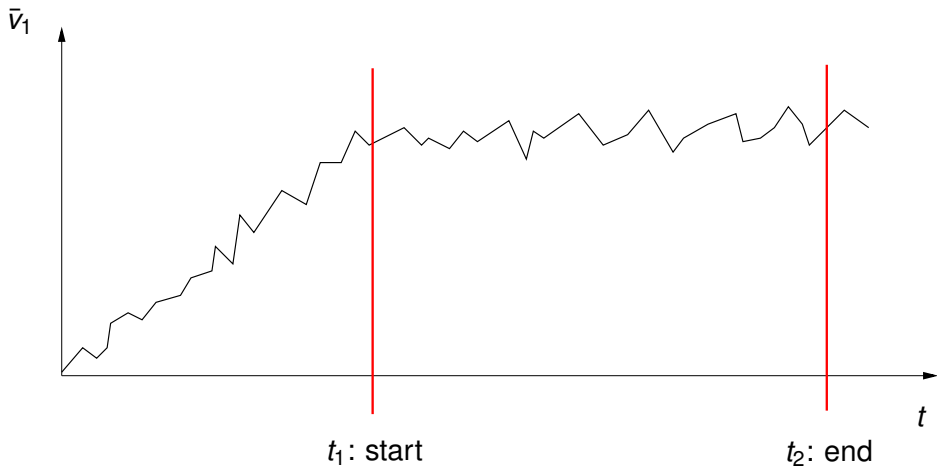
- Flows with large separation
 - Bluff-body flows (e.g. flow around a car); the wake often includes large, unsteady, turbulent structures
 - Transition
- In RANS all turbulent scales are modelled \Rightarrow inaccurate
 - In LES only small, isotropic turbulent scales are modelled \Rightarrow accurate
LES is *very* much more expensive than RANS.

FINITE VOLUME RANS AND LES CODES.

	RANS	LES
Domain	2D or 3D	always 3D
Time domain	steady or unsteady	always unsteady
Space discretization	2nd order upwind	central differencing
Time discretization	1st order	2nd order (e.g. C-N)
Turbulence model	\geq two-equations	zero- or one-eq

TIME AVERAGING IN LES

- t_1 : Start time averaging
- t_2 : Stop time averaging



NEAR-WALL RESOLUTION

- Biggest problem with LES: near walls, it requires very fine mesh in **all** directions, not only in the near-wall direction.

NEAR-WALL RESOLUTION

- Biggest problem with LES: near walls, it requires very fine mesh in **all** directions, not only in the near-wall direction.
- The reason: violent low-speed outward ejections and high-speed in-rushes must be resolved (often called **streaks**).

NEAR-WALL RESOLUTION

- Biggest problem with LES: near walls, it requires very fine mesh in **all** directions, not only in the near-wall direction.
- The reason: violent low-speed outward ejections and high-speed in-rushes must be resolved (often called **streaks**).
- A resolved these structures in LES requires $\Delta x^+ \simeq 100$, $\Delta y_{min}^+ \simeq 1$ and $\Delta z^+ \simeq 30$

NEAR-WALL RESOLUTION

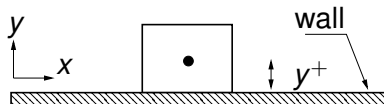
- Biggest problem with LES: near walls, it requires very fine mesh in **all** directions, not only in the near-wall direction.
- The reason: violent low-speed outward ejections and high-speed in-rushes must be resolved (often called **streaks**).
- A resolved these structures in LES requires $\Delta x^+ \simeq 100$, $\Delta y_{min}^+ \simeq 1$ and $\Delta z^+ \simeq 30$
- The object is to develop a near-wall treatment which **models** the streaks (URANS) \Rightarrow much larger Δx and Δz

NEAR-WALL RESOLUTION

- Biggest problem with LES: near walls, it requires very fine mesh in **all** directions, not only in the near-wall direction.
- The reason: violent low-speed outward ejections and high-speed in-rushes must be resolved (often called **streaks**).
- A resolved these structures in LES requires $\Delta x^+ \simeq 100$, $\Delta y_{min}^+ \simeq 1$ and $\Delta z^+ \simeq 30$
- The object is to develop a near-wall treatment which **models** the streaks (URANS) \Rightarrow much larger Δx and Δz
- In the presentation we use Hybrid LES-RANS for which the grid requirements are much smaller than for LES

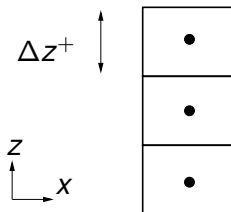
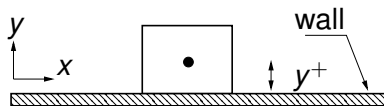
NEAR-WALL RESOLUTION CONT'D

- In RANS when using wall-functions, $30 < y^+ < 100$ for the wall-adjacent cells



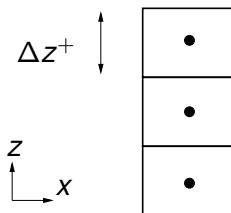
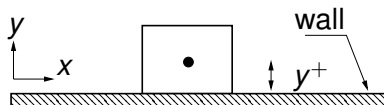
NEAR-WALL RESOLUTION CONT'D

- In RANS when using wall-functions, $30 < y^+ < 100$ for the wall-adjacent cells
- In LES, $\Delta z^+ \simeq 30$



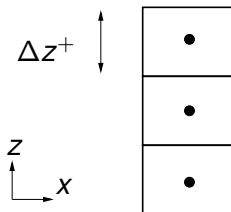
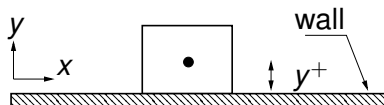
NEAR-WALL RESOLUTION CONT'D

- In RANS when using wall-functions, $30 < y^+ < 100$ for the wall-adjacent cells
- In LES, $\Delta z^+ \simeq 30$
EVERYWHERE

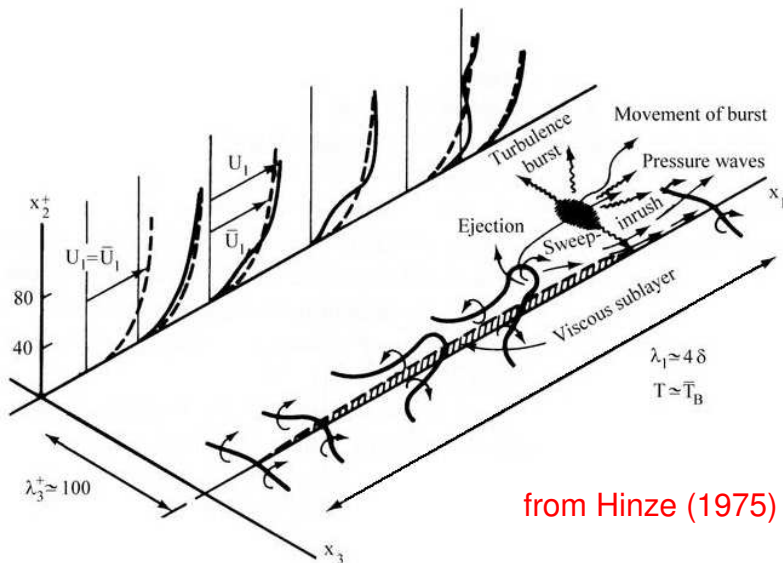


NEAR-WALL RESOLUTION CONT'D

- In RANS when using wall-functions, $30 < y^+ < 100$ for the wall-adjacent cells
- In LES, $\Delta z^+ \simeq 30$
EVERYWHERE
- **AND** $\Delta x^+ \simeq 100$,
 $\Delta y_{min}^+ \simeq 1$

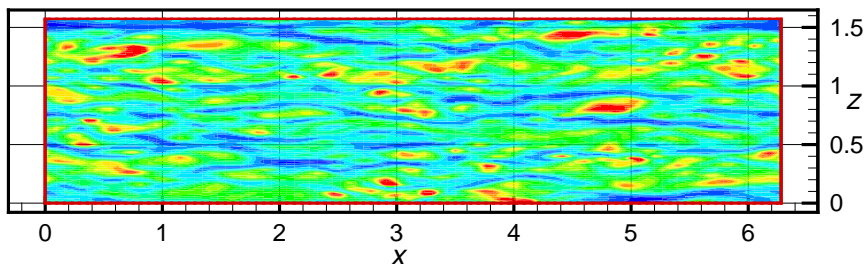


NEAR-WALL TREATMENT



from Hinze (1975)

NEAR-WALL TREATMENT



- Fluctuating streamwise velocity at $y^+ = 5$. DNS of channel flow.
- We find that the structures in the spanwise direction are very small which requires a very **fine** mesh in **z** direction.

ZONAL PANS MODEL

L. Davidson

A New Approach of Zonal Hybrid RANS-LES Based on a Two-equation $k - \varepsilon$ Model [7]

ETMM9, Thessaloniki, 7-9 June 2012

Financed by the EU project

ATAAC (Advanced Turbulence Simulation for Aerodynamic Application Challenges)

DLR, Airbus UK, Alenia, ANSYS, Beijing Tsinghua University, CFS Engineering, Chalmers, Dassault Aviation, EADS, Eurocopter Deutschland, FOI, Imperial College, IMFT, LFK, NLR, NTS, Numeca, ONERA, Rolls-Royce Deutschland, TU Berlin, TU Darmstadt, UniMAN

PANS LOW REYNOLDS NUMBER MODEL [17]

$$\frac{\partial k}{\partial t} + \frac{\partial(kU_j)}{\partial x_j} = \frac{\partial}{\partial x_j} \left[\left(\nu + \frac{\nu_t}{\sigma_{ku}} \right) \frac{\partial k}{\partial x_j} \right] + (P_k - \varepsilon)$$

$$\frac{\partial \varepsilon}{\partial t} + \frac{\partial(\varepsilon U_j)}{\partial x_j} = \frac{\partial}{\partial x_j} \left[\left(\nu + \frac{\nu_t}{\sigma_{\varepsilon u}} \right) \frac{\partial \varepsilon}{\partial x_j} \right] + C_{\varepsilon 1} P_k \frac{\varepsilon}{k} - C_{\varepsilon 2}^* \frac{\varepsilon^2}{k}$$

$$\nu_t = C_\mu f_\mu \frac{k^2}{\varepsilon}, C_{\varepsilon 2}^* = C_{\varepsilon 1} + \frac{f_k}{f_\varepsilon} (C_{\varepsilon 2} f_2 - C_{\varepsilon 1}), \sigma_{ku} \equiv \sigma_k \frac{f_k^2}{f_\varepsilon}, \sigma_{\varepsilon u} \equiv \sigma_\varepsilon \frac{f_k^2}{f_\varepsilon}$$

$C_{\varepsilon 1}$, $C_{\varepsilon 2}$, σ_k , σ_ε and C_μ same values as [1]. $f_\varepsilon = 1$. f_2 and f_μ read

$$f_2 = \left[1 - \exp\left(-\frac{y^*}{3.1}\right) \right]^2 \left\{ 1 - 0.3 \exp\left[-\left(\frac{R_t}{6.5}\right)^2\right] \right\}$$

$$f_\mu = \left[1 - \exp\left(-\frac{y^*}{14}\right) \right]^2 \left\{ 1 + \frac{5}{R_t^{3/4}} \exp\left[-\left(\frac{R_t}{200}\right)^2\right] \right\}$$

- Baseline model: $f_k = 0.4$. Range of $0.2 < f_k < 0.6$ is evaluated

PANS LOW REYNOLDS NUMBER MODEL [17]

$$\frac{\partial k}{\partial t} + \frac{\partial(kU_j)}{\partial x_j} = \frac{\partial}{\partial x_j} \left[\left(\nu + \frac{\nu_t}{\sigma_{ku}} \right) \frac{\partial k}{\partial x_j} \right] + (P_k - \varepsilon)$$

$$\frac{\partial \varepsilon}{\partial t} + \frac{\partial(\varepsilon U_j)}{\partial x_j} = \frac{\partial}{\partial x_j} \left[\left(\nu + \frac{\nu_t}{\sigma_{\varepsilon u}} \right) \frac{\partial \varepsilon}{\partial x_j} \right] + C_{\varepsilon 1} P_k \frac{\varepsilon}{k} - C_{\varepsilon 2}^* \frac{\varepsilon^2}{k}$$

$$\nu_t = C_\mu f_\mu \frac{k^2}{\varepsilon}, \quad C_{\varepsilon 2}^* = C_{\varepsilon 1} + \frac{f_k}{f_\varepsilon} (C_{\varepsilon 2} f_2 - C_{\varepsilon 1}), \quad \sigma_{ku} \equiv \sigma_k \frac{f_k^2}{f_\varepsilon}, \quad \sigma_{\varepsilon u} \equiv \sigma_\varepsilon \frac{f_k^2}{f_\varepsilon}$$

$C_{\varepsilon 1}$, $C_{\varepsilon 2}$, σ_k , σ_ε and C_μ same values as [1]. $f_\varepsilon = 1$. f_2 and f_μ read

$$f_2 = \left[1 - \exp\left(-\frac{y^*}{3.1}\right) \right]^2 \left\{ 1 - 0.3 \exp\left[-\left(\frac{R_t}{6.5}\right)^2\right] \right\}$$

$$f_\mu = \left[1 - \exp\left(-\frac{y^*}{14}\right) \right]^2 \left\{ 1 + \frac{5}{R_t^{3/4}} \exp\left[-\left(\frac{R_t}{200}\right)^2\right] \right\}$$

- Baseline model: $f_k = 0.4$. Range of $0.2 < f_k < 0.6$ is evaluated

PANS LOW REYNOLDS NUMBER MODEL [17]

$$\frac{\partial k}{\partial t} + \frac{\partial(kU_j)}{\partial x_j} = \frac{\partial}{\partial x_j} \left[\left(\nu + \frac{\nu_t}{\sigma_{ku}} \right) \frac{\partial k}{\partial x_j} \right] + (P_k - \varepsilon)$$

$$\frac{\partial \varepsilon}{\partial t} + \frac{\partial(\varepsilon U_j)}{\partial x_j} = \frac{\partial}{\partial x_j} \left[\left(\nu + \frac{\nu_t}{\sigma_{\varepsilon u}} \right) \frac{\partial \varepsilon}{\partial x_j} \right] + C_{\varepsilon 1} P_k \frac{\varepsilon}{k} - C_{\varepsilon 2}^* \frac{\varepsilon^2}{k}$$

$$\nu_t = C_{\mu} f_{\mu} \frac{k^2}{\varepsilon}, \quad C_{\varepsilon 2}^* = 1.5 + \frac{f_k}{f_{\varepsilon}} (1.9 - 1.5), \quad \sigma_{ku} \equiv \sigma_k \frac{f_k^2}{f_{\varepsilon}}, \quad \sigma_{\varepsilon u} \equiv \sigma_{\varepsilon} \frac{f_k}{f_{\varepsilon}}$$

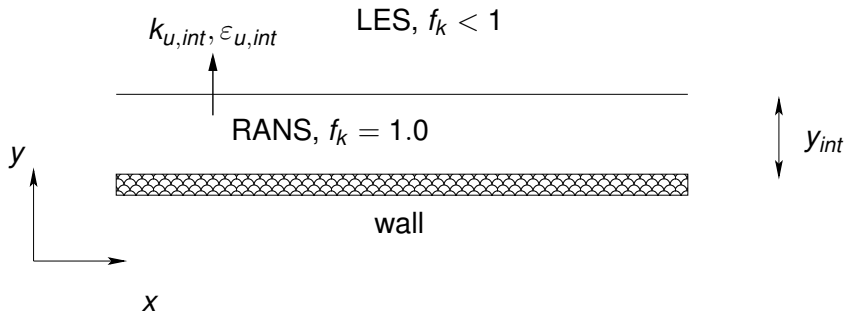
$C_{\varepsilon 1}$, $C_{\varepsilon 2}$, σ_k , σ_{ε} and C_{μ} same values as [1]. $f_{\varepsilon} = 1$. f_2 and f_{μ} read

$$f_2 = \left[1 - \exp\left(-\frac{y^*}{3.1}\right) \right]^2 \left\{ 1 - 0.3 \exp\left[-\left(\frac{R_t}{6.5}\right)^2\right] \right\}$$

$$f_{\mu} = \left[1 - \exp\left(-\frac{y^*}{14}\right) \right]^2 \left\{ 1 + \frac{5}{R_t^{3/4}} \exp\left[-\left(\frac{R_t}{200}\right)^2\right] \right\}$$

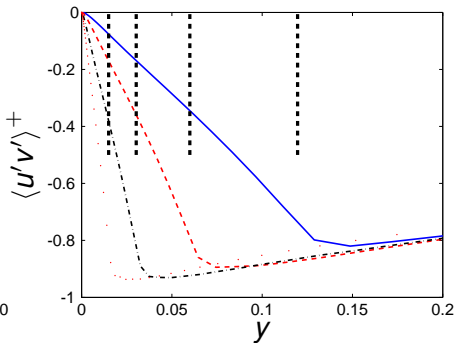
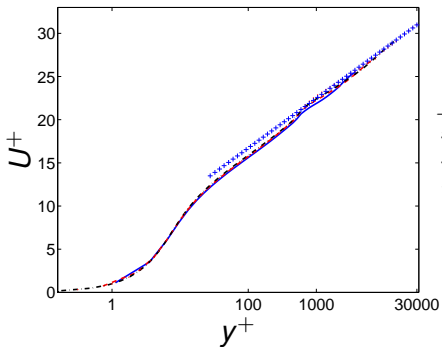
- Baseline model: $f_k = 0.4$. Range of $0.2 < f_k < 0.6$ is evaluated

CHANNEL FLOW: ZONAL RANS-LES



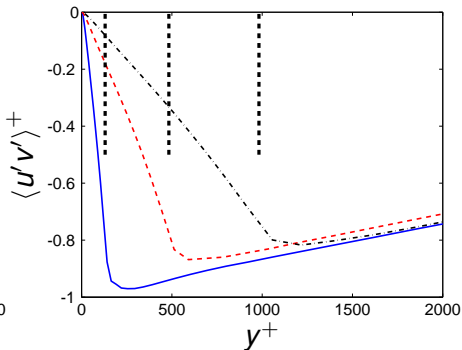
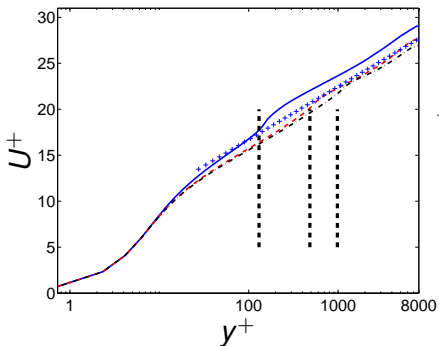
- **Interface:** how to treat k and ϵ over the interface? They should be reduced from their RANS values to suitable LES values
- The usual convection and diffusion across the interface is cut off, and new “interface boundary” conditions are prescribed
- $k_{u,int} = f_k k_{RANS}$
- Nothing is done for ϵ
- $x_{max} = 3.2$ (64 cells), $z_{max} = 1.6$ (64 cells), y dir: 80 – 128 cells
- CDS in entire region

$$(N_x \times N_z) = (64 \times 64). \quad y_{int}^+ = 500$$



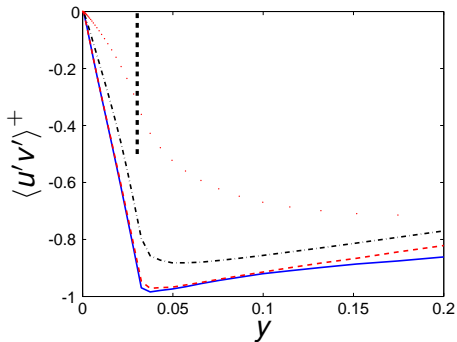
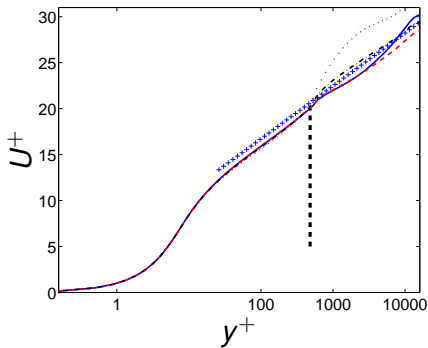
— $Re_\tau = 4000$
 - - - $Re_\tau = 8000$
 - . - . $Re_\tau = 16000$;
 $Re_\tau = 32000$.

INTERFACE LOCATION. $Re_\tau = 8000$.



— $y^+ = 130$ - - - $y^+ = 500$ - . - $y^+ = 980$

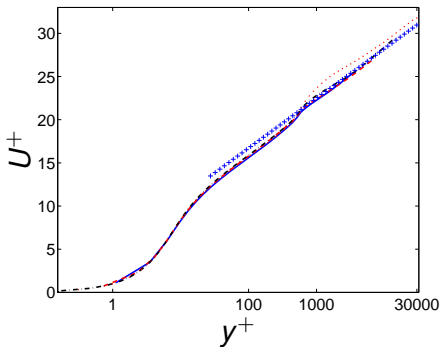
EFFECT OF f_k . $Re_\tau = 16\,000$. $y_{int}^+ = 500$



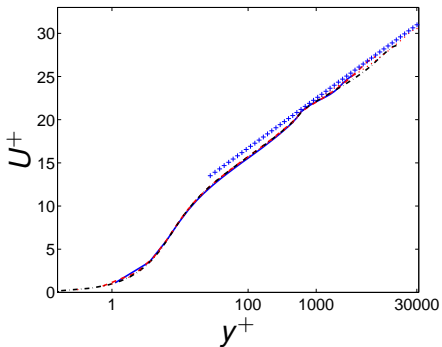
— $f_k = 0.2$ - - - $f_k = 0.3$ - . - $f_k = 0.5$. . . $f_k = 0.6$

EFFECT OF RESOLUTION: VELOCITY

$(N_x \times N_z) = (32 \times 32)$

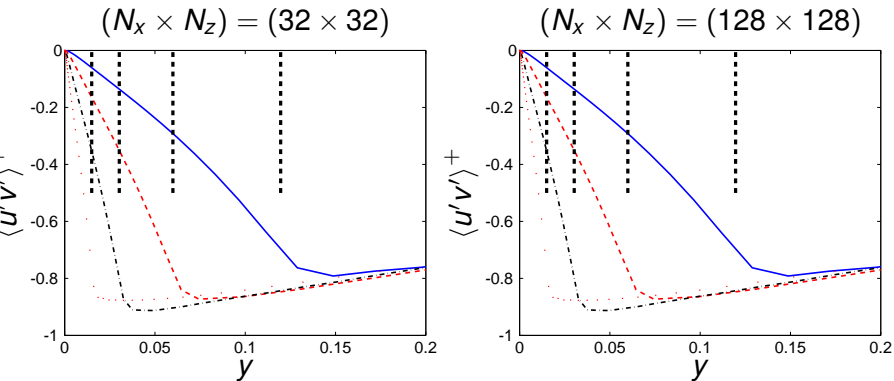


$(N_x \times N_z) = (128 \times 128)$



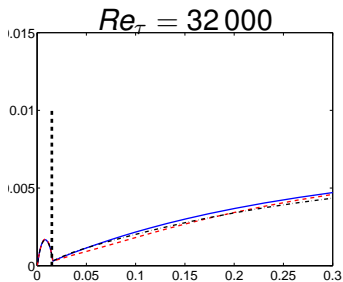
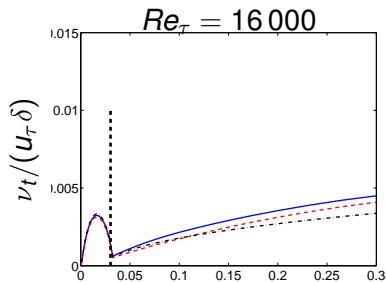
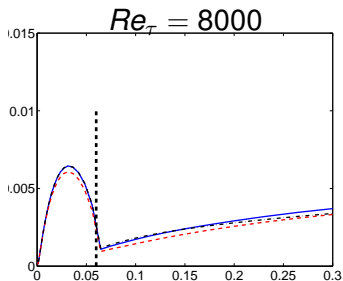
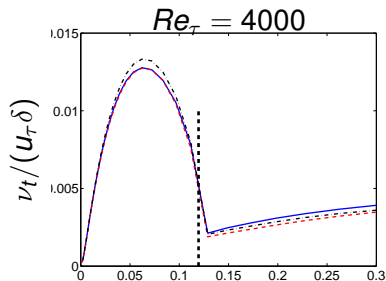
— $Re_\tau = 4000$ - - - $Re_\tau = 8000$ - . - . $Re_\tau = 16000$;
..... $Re_\tau = 32000$.

EFFECT OF RESOLUTION: RESOLVED SHEAR STRESS



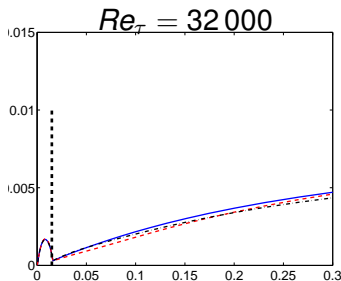
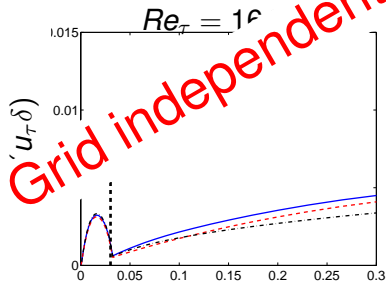
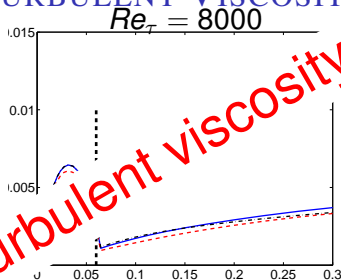
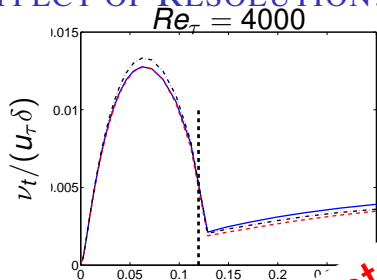
— $Re_\tau = 4000$ - - - $Re_\tau = 8000$ - . - . $Re_\tau = 16000$;
..... $Re_\tau = 32000$.

EFFECT OF RESOLUTION: TURBULENT VISCOSITY



— $(N_x \times N_z) \stackrel{y}{=} 64 \times 64$
- - - 32×32
— 128×128

EFFECT OF RESOLUTION: TURBULENT VISCOSITY



Grid independent turbulent viscosity!

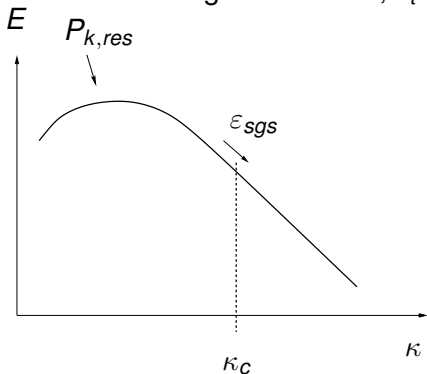
— $(N_x \times N_z) = 64 \times 64$
- - - 32×32
- - - 128×128

SGS MODELS BASED ON GRID SIZE

- When the grid is refined, ν_t gets **smaller**

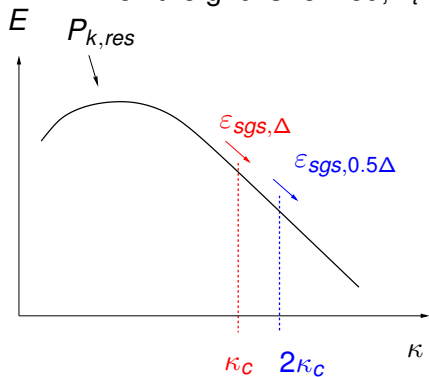
SGS MODELS BASED ON GRID SIZE

- When the grid is refined, ν_t gets **smaller**



SGS MODELS BASED ON GRID SIZE

- When the grid is refined, ν_t gets **smaller**



SGS MODELS BASED ON GRID SIZE

- When the grid is refined, ν_t gets **smaller**

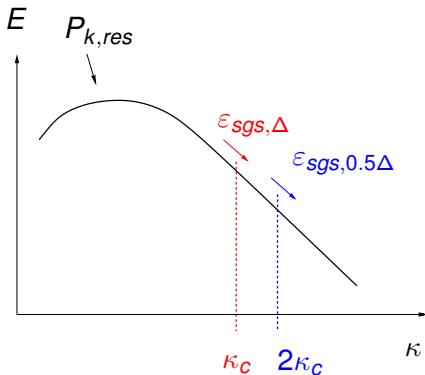
- $\epsilon_{sgs,\Delta} = \epsilon_{sgs,0.5\Delta}$

- $\epsilon_{sgs} = 2\langle \nu_t \bar{s}_{ij} \bar{s}_{ij} \rangle - \langle \tau_{12,t} \rangle \frac{\partial \langle \bar{u} \rangle}{\partial y}$

- Grid refinement \Rightarrow must be accompanied with larger $\bar{s}_{ij} \bar{s}_{ij}$

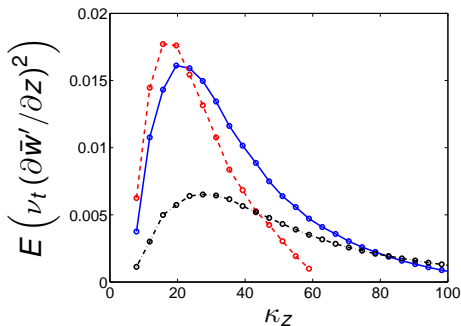
- $\Rightarrow \bar{s}_{ij} \bar{s}_{ij}$ must take place at higher wavenumbers

- if not \Rightarrow **grid dependent**

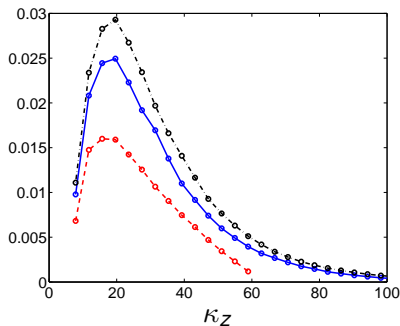


POWER DENSITY SPECTRA OF $\nu_t^{0.5} \frac{\partial \bar{w}'}{\partial z}$

One-eq k_{SGS} model



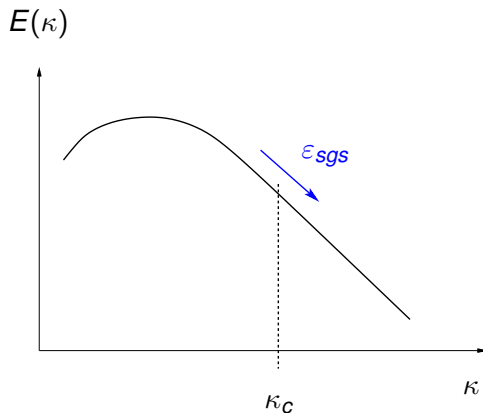
Zonal PANS



— $(N_x \times N_z) = 64 \times 64$
- - - 32×32
- . - . 128×128

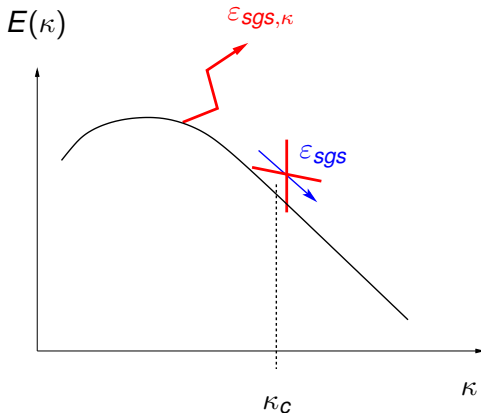
SGS DISSIPATION VS. WAVENUMBER

- Energy spectra of the SGS dissipation show that the peak takes place at **surprisingly** low wavenumber (length scale corresponding to 10 cells or more).



SGS DISSIPATION VS. WAVENUMBER

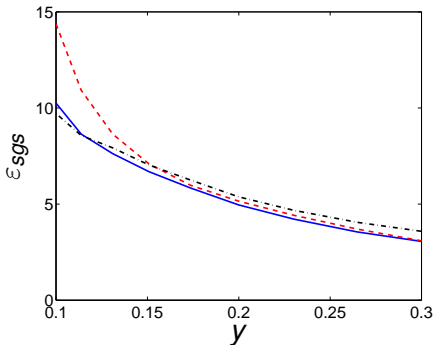
- Energy **spectra** of the SGS dissipation show that the peak takes place at **surprisingly** low wavenumber (length scale corresponding to 10 cells or more).



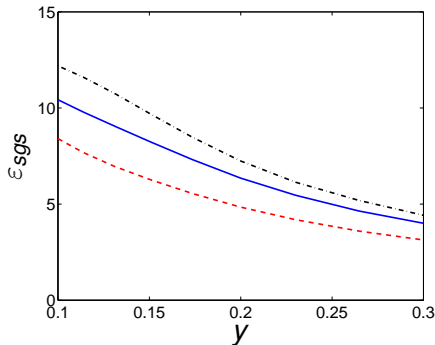
SGS DISSIPATION, $Re_\tau = 8000$

- SGS dissipation in the $\bar{u}'_i \bar{u}'_i / 2$ eq, $\varepsilon_{sgs} = 2 \langle \nu_t \bar{s}_{ij} \bar{s}_{ij} \rangle - \langle \tau_{12,t} \rangle \frac{\partial \langle \bar{u} \rangle}{\partial y}$

One-eq k_{sgs} model



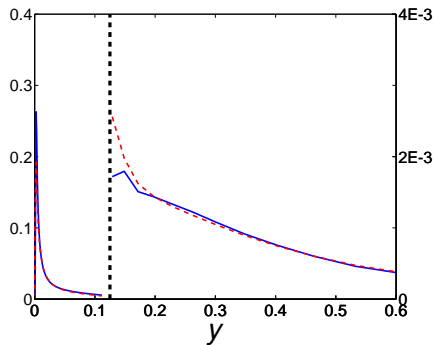
Zonal PANS



— $(N_x \times N_z) = 64 \times 64$ - - - 32×32 - . - 128×128

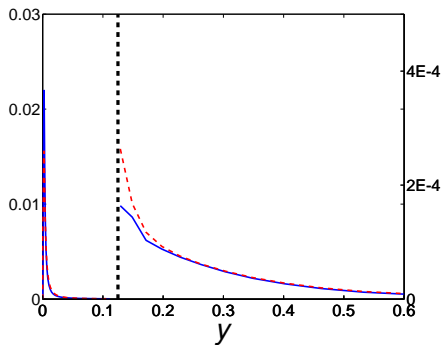
LOCAL EQUILIBRIUM. $Re_\tau = 4000$, $N_x \times N_z = 64 \times 64$.

k equation



— $\langle P_k \rangle^+$
 - - - $\langle \varepsilon \rangle^+$

ε equation



— $\langle C_{\varepsilon 1} P_k / \varepsilon \rangle^+$
 - - - $\langle C_{\varepsilon 2} \varepsilon^2 / k \rangle^+$

Left vertical axes: URANS region; right vertical axes: LES region.

LOCAL EQUILIBRIUM IN ε EQUATION.

- How can both the k eq. and ε be in local equilibrium??

LOCAL EQUILIBRIUM IN ε EQUATION.

- **How** can both the k eq. and ε be in local equilibrium??

If

$$\langle P_k \rangle = \langle \varepsilon \rangle$$

LOCAL EQUILIBRIUM IN ε EQUATION.

- How can both the k eq. and ε be in local equilibrium??

If

$$\langle P_k \rangle = \langle \varepsilon \rangle$$

then

$$C_1 \frac{\langle \varepsilon \rangle}{\langle k \rangle} \langle P_k \rangle \neq C_2^* \frac{\langle \varepsilon \rangle^2}{\langle k \rangle}, \text{ because } C_1 \neq C_2^*$$

LOCAL EQUILIBRIUM IN ε EQUATION.

- How can both the k eq. and ε be in local equilibrium??

If

$$\langle P_k \rangle = \langle \varepsilon \rangle$$

then

$$C_1 \frac{\langle \varepsilon \rangle}{\langle k \rangle} \langle P_k \rangle \neq C_2^* \frac{\langle \varepsilon \rangle^2}{\langle k \rangle}, \text{ because } C_1 \neq C_2^*$$

However, the previous slide shows

$$C_1 \left\langle \frac{\varepsilon}{k} P_k \right\rangle = C_2^* \left\langle \frac{\varepsilon^2}{k} \right\rangle$$

LOCAL EQUILIBRIUM IN ε EQUATION.

- **How** can both the k eq. and ε be in local equilibrium??

If

$$\langle P_k \rangle = \langle \varepsilon \rangle$$

then

$$C_1 \frac{\langle \varepsilon \rangle}{\langle k \rangle} \langle P_k \rangle \neq C_2^* \frac{\langle \varepsilon \rangle^2}{\langle k \rangle}, \text{ because } C_1 \neq C_2^*$$

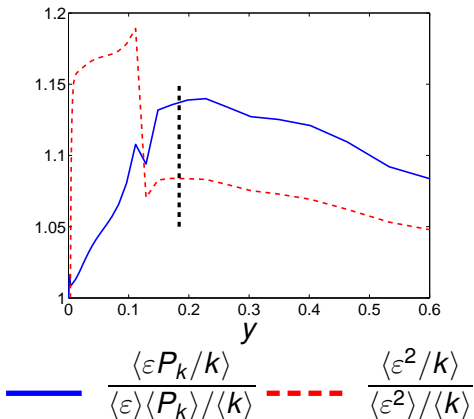
However, the previous slide shows

$$C_1 \left\langle \frac{\varepsilon}{k} P_k \right\rangle = C_2^* \left\langle \frac{\varepsilon^2}{k} \right\rangle$$

- **Answer:** when time-averaging $\langle ab \rangle \neq \langle a \rangle \langle b \rangle$

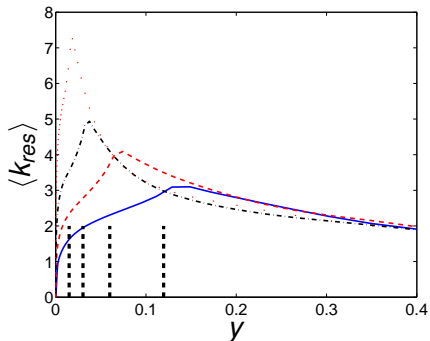
LOCAL EQUILIBRIUM IN ε EQUATION.

- The answer is because of time averaging ($\langle ab \rangle < \langle a \rangle \langle b \rangle$), (see below)

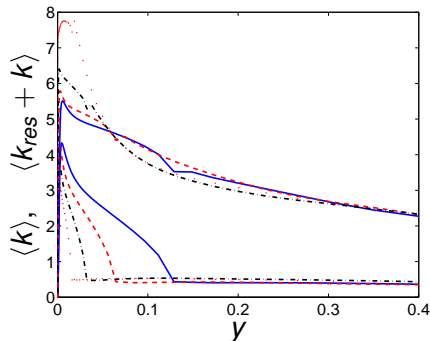


RESOLVED AND MODELLED TURBULENT KINETIC ENERGY.

Resolved



Modelled: bottom; total: top



— $Re_\tau = 4000$ - - - $Re_\tau = 8000$ - . - $Re_\tau = 16000$;
· · · $Re_\tau = 32000$.

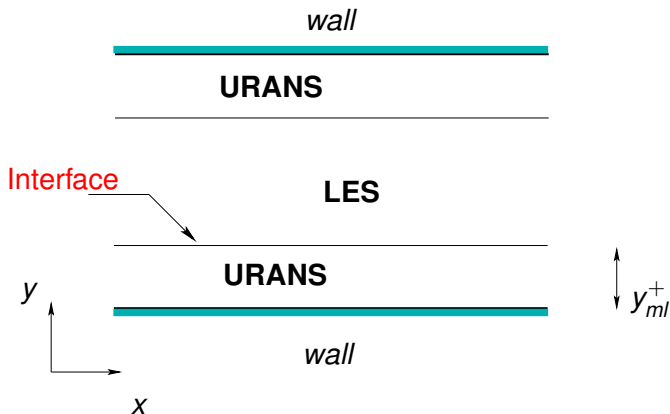
CONCLUDING REMARKS

- LRN PANS works well as zonal LES-RANS model for very high Re_τ ($> 32\,000$)
- The model gives **grid independent** results
- The location of the interface is not important (it should not be too close to the wall)
- Values of $0.2 < f_k < 0.5$ have little impact on the results

HYBRID LES-RANS

Near walls: a RANS one-eq. k or a $k - \omega$ model.

In core region: a LES one-eq. k_{SGS} model.



- Location of **interface** either pre-defined or automatically computed

MOMENTUM EQUATIONS

- The Navier-Stokes, time-averaged in the near-wall regions and filtered in the core region, reads

$$\frac{\partial \bar{u}_i}{\partial t} + \frac{\partial}{\partial x_j} (\bar{u}_i \bar{u}_j) = -\frac{1}{\rho} \frac{\partial \bar{p}}{\partial x_i} + \frac{\partial}{\partial x_j} \left[(\nu + \nu_T) \frac{\partial \bar{u}_i}{\partial x_j} \right]$$

$$\nu_T = \nu_t, Y \leq Y_{ml}$$

$$\nu_T = \nu_{sgs}, Y \geq Y_{ml}$$

- The equation above: **URANS** or **LES**? Same boundary conditions \Rightarrow same solution!

TURBULENCE MODEL

- Use one-equation model in both URANS region and LES region.

$$\frac{\partial k_T}{\partial t} + \frac{\partial}{\partial x_j} (\bar{u}_j k_T) = \frac{\partial}{\partial x_j} \left[(\nu + \nu_T) \frac{\partial k_T}{\partial x_j} \right] + P_{k_T} - C_\epsilon \frac{k_T^{3/2}}{\ell}$$

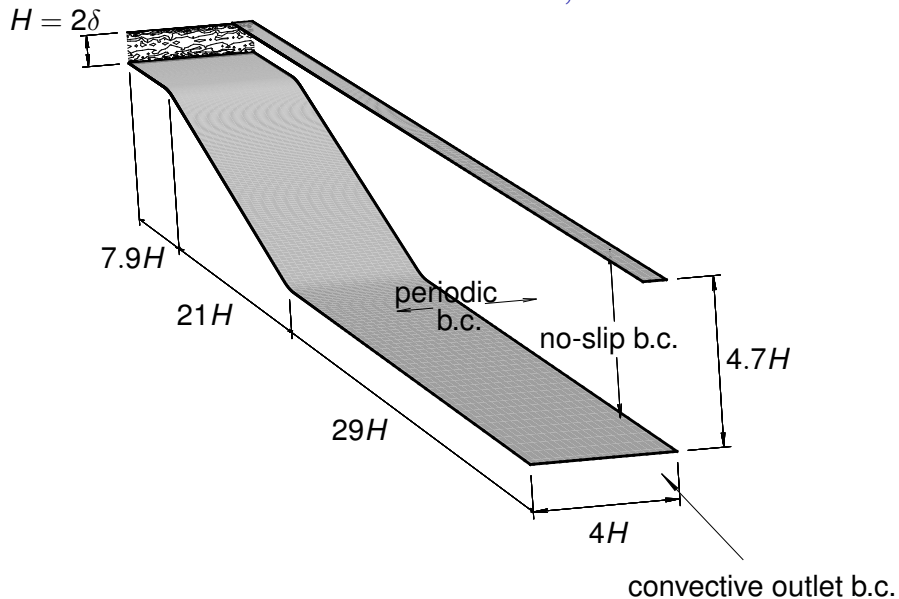
$$P_{k_T} = 2\nu_T \bar{S}_{ij} \bar{S}_{ij}, \quad \nu_T = C_k \ell k_T^{1/2}$$

- **LES**-region: $k_T = k_{sgs}$, $\nu_T = \nu_{sgs}$, $\ell = \Delta = (\delta V)^{1/3}$
- **URANS**-region: $k_T = k$, $\nu_T = \nu_t$,
 $\ell \equiv \ell_{RANS} = 2.5\eta[1 - \exp(-Ak^{1/2}y/\nu)]$, Chen-Patel model (AIAA J. 1988)
- Location of **interface** can be defined by $\min(0.65\Delta, y)$,
 $\Delta = \max(\Delta x, \Delta y, \Delta z)$

DIFFUSER[9]

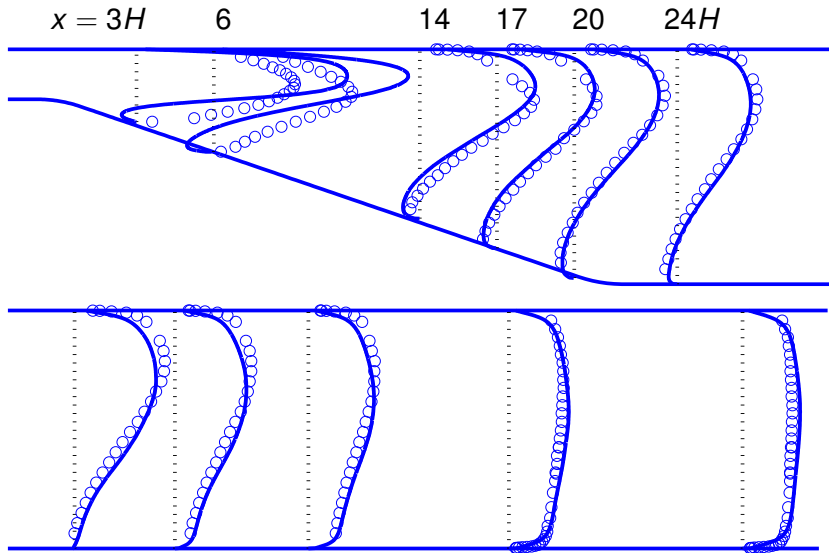
- Instantaneous inlet data from channel DNS used.
- Domain: $-8 \leq x \leq 48$, $0 \leq y_{inlet} \leq 1$, $0 \leq z \leq 4$.
- $x_{max} = 40$ gave return flow at the outlet
- Grid: $258 \times 66 \times 32$.
- $Re = U_{in}H/\nu = 18\,000$, angle 10°
- The grid is much too coarse for LES (in the inlet region $\Delta z^+ \simeq 170$)
- Matching plane fixed at y_{ml} at the inlet. In the diffuser it is located along the 2D instantaneous **streamline** corresponding to y_{ml} .

DIFFUSER GEOMETRY. $Re = 18\ 000$, ANGLE 10°



DIFFUSER: RESULTS WITH LES

- Velocities. Markers: experiments by Buice & Eaton (1997)



DIFFUSER: RESULTS WITH RANS-LES

$x = 3H$

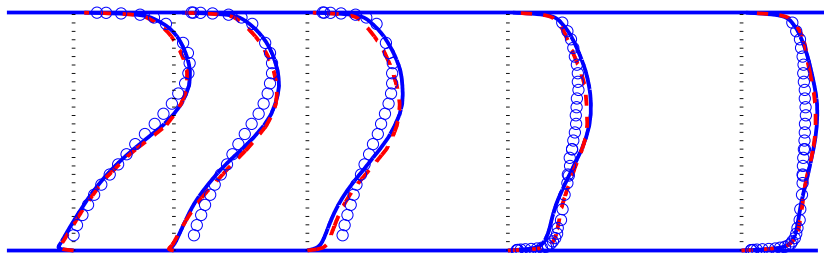
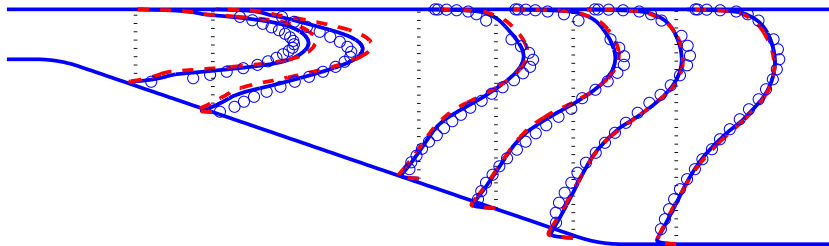
6

14

17

20

24H



$x/H = 27$

30

34

40

47H

forcing: 

no forcing 

SHEAR STRESSES ($\times 2$ IN LOWER HALF)

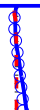
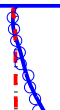
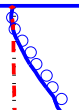
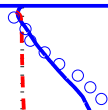
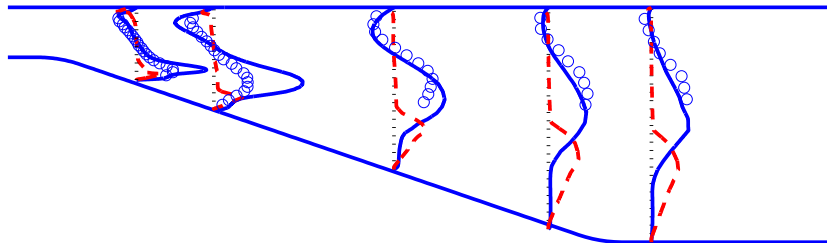
$x = 3H$

6

13

19

$23H$



$x/H = 26$

33

40

$47H$

resolved; modelled

RANS-LES: ν_t/ν

$x = 3H$

6

14

17

20

24H

At $x = -7H$ $\nu_{T,max}/\nu \simeq 11$

At $x = 24H$, $\nu_{T,max}/\nu \simeq 450$

$x/H = 27$

30

34

40

47H

— forcing; - - - no forcing

$k - \omega$ MODEL SST-DES

- DES [24]: **D**etached **E**ddy **S**imulation
- SST [18, 19]: A combination of the $k - \varepsilon$ and the $k - \omega$ model

$$\frac{\partial k}{\partial t} + \frac{\partial}{\partial x_j}(\bar{u}_j k) = \frac{\partial}{\partial x_j} \left[\left(\nu + \frac{\nu_t}{\sigma_k} \right) \frac{\partial k}{\partial x_j} \right] + P_k - \beta^* k \omega$$
$$\frac{\partial \omega}{\partial t} + \frac{\partial}{\partial x_j}(\bar{u}_j \omega) = \frac{\partial}{\partial x_j} \left[\left(\nu + \frac{\nu_t}{\sigma_\omega} \right) \frac{\partial \omega}{\partial x_j} \right] + \alpha \frac{P_k}{\nu_t} - \beta \omega^2 + \dots$$

- The dissipation term in the k equation is modified as [19, 25]

$$\beta^* k \omega \rightarrow \beta^* k \omega F_{DES}, \quad F_{DES} = \max \left\{ \frac{L_t}{C_{DES} \Delta}, 1 \right\}$$
$$\Delta = \max \{ \Delta x_1, \Delta x_2, \Delta x_3 \}, \quad L_t = \frac{k^{1/2}}{\beta^* \omega}$$

⇒ RANS near walls and LES away from walls

RESOLUTION

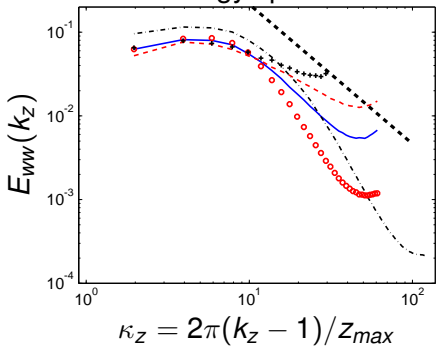
- For the near-wall region, we know how fine the mesh should be in terms of viscous units (see Slide 22)
- An appropriate resolution for the fully turbulent part of the boundary layer is $\delta/\Delta x \simeq 10 - 20$ and $\delta/\Delta z \simeq 20 - 40$
- This may be relevant also for jets and shear layers

HOW TO ESTIMATE RESOLUTION IN GENERAL? [4, 5]

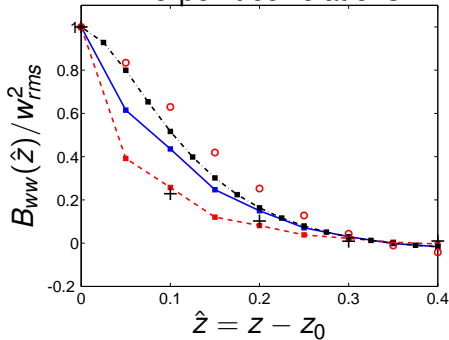
- **Energy** spectra (both in spanwise direction and time)
- **Two-point** correlations
- Ratio of SGS turbulent kinetic energy $\langle k_{sgs} \rangle$ to resolved $0.5\langle u'u' + v'v' + w'w' \rangle$
- Ratio of SGS shear stress $\langle \tau_{sgs,12} \rangle$ to resolved $\langle u'v' \rangle$
- Ratio of SGS viscosity, $\langle \nu_{sgs} \rangle$ to molecular, ν
- Energy spectra of **SGS dissipation**
- Comparison of SGS dissipation due to $\partial u'_i / \partial x_j$ and $\partial \langle \bar{u}_i \rangle / \partial x_j$

CHANNEL FLOW, $Re_\tau = 4000$, $y^+ = 440$

Energy spectra



Two-point correlations

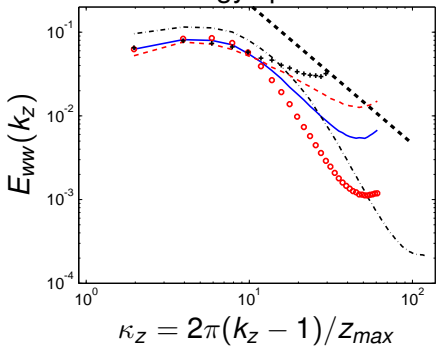


—■ $(\Delta x, \Delta z)$
 - - -■ $0.5\Delta x$
 - · - -■ $0.5\Delta z$
 · · · · ·○ $2\Delta x$;
 +·+·+· $2\Delta z$

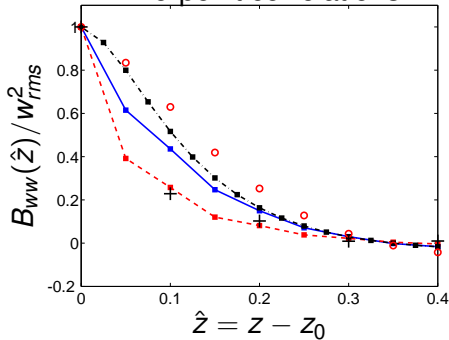
The $(\Delta x, \Delta z)$ mesh is $(\delta/\Delta x, \delta/\Delta z) = (10, 20)$

CHANNEL FLOW, $Re_\tau = 4000$, $y^+ = 440$

Energy spectra



Two-point correlations



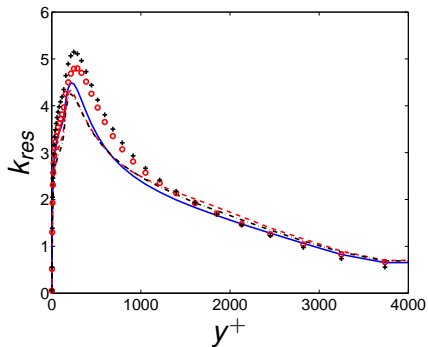
—■ $(\Delta x, \Delta z)$
 - -■ $0.5\Delta x$
 - · -■ $0.5\Delta z$
 ○ $2\Delta x$;
 + $2\Delta z$

The $(\Delta x, \Delta z)$ mesh is $(\delta/\Delta x, \delta/\Delta z) = (10, 20)$

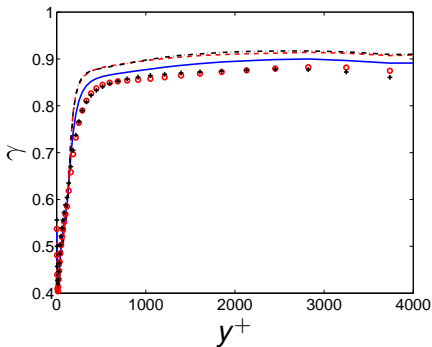
- **Two-point correlation** is better
- Shows that $2\Delta z$ and $2\Delta x$ (two-point corr in x) are too coarse.

CHANNEL FLOW, $Re_\tau = 4000$, $y^+ = 440$

$$k_{res} = (u'^2 + v'^2 + w'^2)/2$$



$$\gamma = \frac{k_{res}}{\langle k_T \rangle + k_{res}}$$

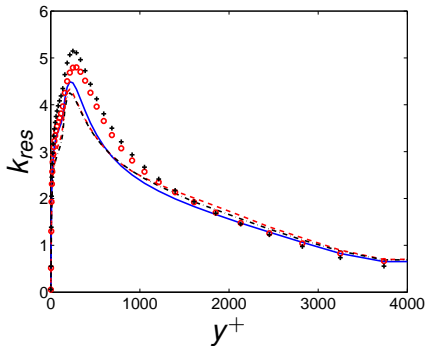


• Pope [20] suggests $\gamma > 0.8$ indicates well resolved flow

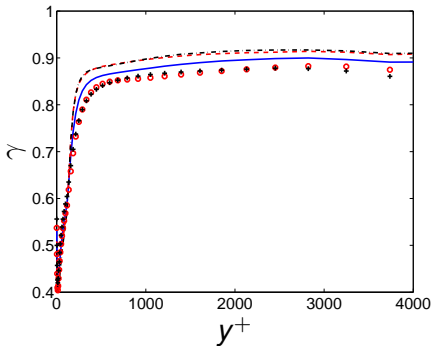
— $(\Delta x, \Delta z)$ - - - $0.5\Delta x$ - . - $0.5\Delta z$ ○ $2\Delta x$; +: $2\Delta z$

CHANNEL FLOW, $Re_\tau = 4000$, $y^+ = 440$

$$k_{res} = (u'^2 + v'^2 + w'^2)/2$$



$$\gamma = \frac{k_{res}}{\langle k_T \rangle + k_{res}}$$

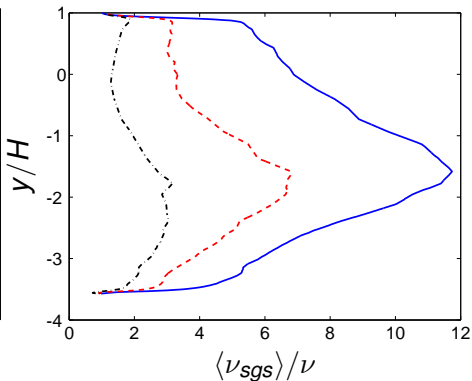
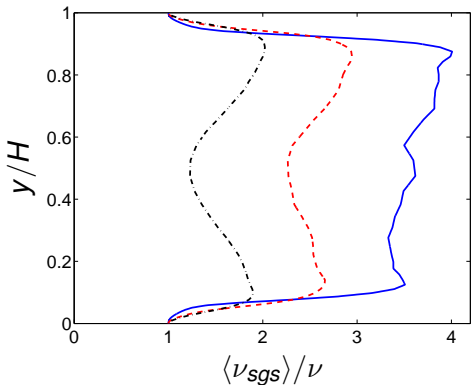
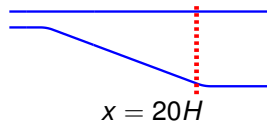
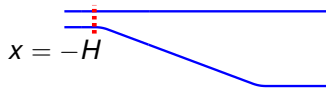


- Pope [20] suggests $\gamma > 0.8$ indicates well resolved flow

— $(\Delta x, \Delta z)$ - - - $0.5\Delta x$ - . - $0.5\Delta z$ \circ $2\Delta x$; +: $2\Delta z$

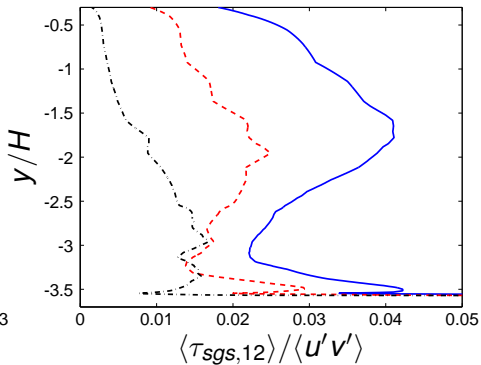
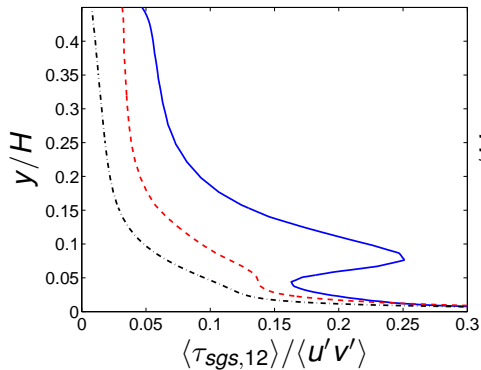
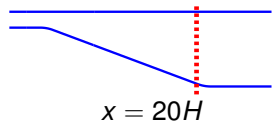
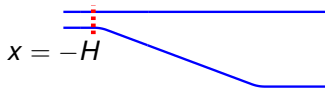
- **Pope criterion** does not work here

SGS vs. MOLECULAR VISCOSITY [5]



— $N_z = 32$; - - - $N_z = 64$; - · - $N_z = 128$.

SGS VS. RESOLVED SHEAR STRESSES



— $N_z = 32$;
 - - - $N_z = 64$;
 - · - · $N_z = 128$.

THE PANS MODEL

- The PANS model is a modified $k - \varepsilon$ model
- It can operate both in RANS mode and LES mode
- In the present work a low-Reynolds turbulence version of the PANS is used
- A method how to implement embedded LES is proposed
- It is evaluated for channel flow and hump flow

Embedded LES Using PANS [10, 11]
Lars Davidson¹ and Shia-Hui Peng^{1,2}
Davidson & Peng

¹Department of Applied Mechanics
Chalmers University of Technology, SE-412 96 Gothenburg, SWEDEN
²FOI, Swedish Defence Research Agency, SE-164 90, Stockholm,
SWEDEN

PANS LOW REYNOLDS NUMBER MODEL [17]

$$\frac{\partial k_u}{\partial t} + \frac{\partial(k_u U_j)}{\partial x_j} = \frac{\partial}{\partial x_j} \left[\left(\nu + \frac{\nu_u}{\sigma_{ku}} \right) \frac{\partial k_u}{\partial x_j} \right] + (P_u - \varepsilon_u)$$

$$\frac{\partial \varepsilon_u}{\partial t} + \frac{\partial(\varepsilon_u U_j)}{\partial x_j} = \frac{\partial}{\partial x_j} \left[\left(\nu + \frac{\nu_u}{\sigma_{\varepsilon u}} \right) \frac{\partial \varepsilon_u}{\partial x_j} \right] + C_{\varepsilon 1} P_u \frac{\varepsilon_u}{k_u} - C_{\varepsilon 2}^* \frac{\varepsilon_u^2}{k_u}$$

$$\nu_u = C_\mu f_\mu \frac{k_u^2}{\varepsilon_u}, C_{\varepsilon 2}^* = C_{\varepsilon 1} + \frac{f_k}{f_\varepsilon} (C_{\varepsilon 2} f_2 - C_{\varepsilon 1}), \sigma_{ku} \equiv \sigma_k \frac{f_k^2}{f_\varepsilon}, \sigma_{\varepsilon u} \equiv \sigma_\varepsilon \frac{f_k^2}{f_\varepsilon}$$

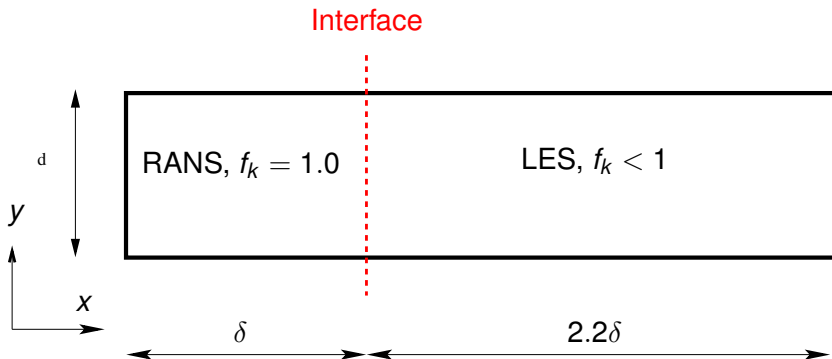
$C_{\varepsilon 1}$, $C_{\varepsilon 2}$, σ_k , σ_ε and C_μ same values as [1]. $f_\varepsilon = 1$. f_2 and f_μ read

$$f_2 = \left[1 - \exp\left(-\frac{y^*}{3.1}\right) \right]^2 \left\{ 1 - 0.3 \exp\left[-\left(\frac{R_t}{6.5}\right)^2\right] \right\}$$

$$f_\mu = \left[1 - \exp\left(-\frac{y^*}{14}\right) \right]^2 \left\{ 1 + \frac{5}{R_t^{3/4}} \exp\left[-\left(\frac{R_t}{200}\right)^2\right] \right\}$$

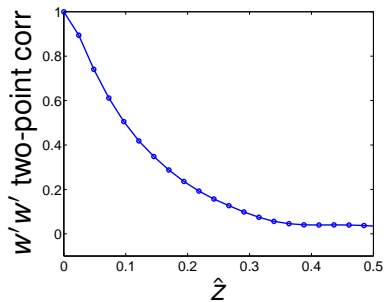
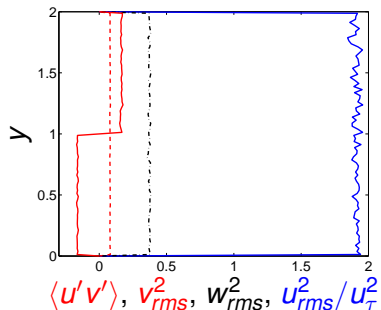
- Baseline model: $f_k = 0.4$. Range of $0.2 < f_k < 0.6$ is evaluated

CHANNEL FLOW: DOMAIN



- **Interface:** Synthetic turbulent fluctuations are introduced as additional **convective** fluxes in the **momentum** equations and the **continuity** equation
- $f_k = 0.4$ is the baseline value for LES [17]

INLET FLUCTUATIONS



- Anisotropic synthetic fluctuations, u' , v' , w' ,
- Integral length scale $\mathcal{L} \simeq 0.13$ (see 2-p point correlation)
- Asymmetric time filter $(u')^m = a(u')^{m-1} + b(u')^m$ with $a = 0.954$, $b = (1 - a^2)^{1/2}$ gives a time integral scale $\mathcal{T} = 0.015$ ($\Delta t = 0.00063$)

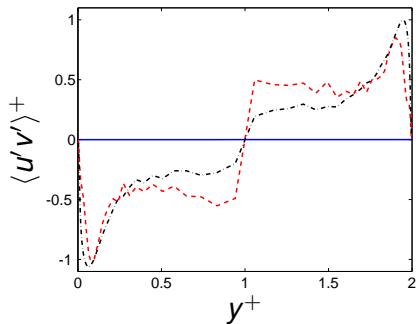
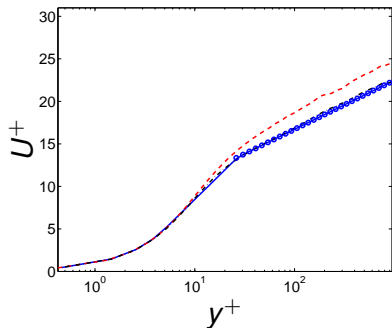
INTERFACE CONDITIONS FOR k_u AND ε_u

- For k_u & ε_u we prescribe “inlet” boundary conditions at the interface.
- First, the usual convective and diffusive fluxes at the interface are set to zero
- Next, new convective fluxes are added. Which “inlet” values should be used at the interface?
 - ▶ $k_{u,int} = f_k k_{RANS}(x = 0.5\delta)$, $\varepsilon_{u,int} = C_\mu^{3/4} k_{u,int}^{3/2} / \ell_{sgs}$, $\ell_{sgs} = C_s \Delta$,
 $\Delta = V^{1/3}$
 - ▶

INTERFACE CONDITIONS FOR k_U AND ε_U

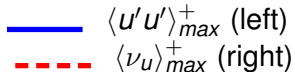
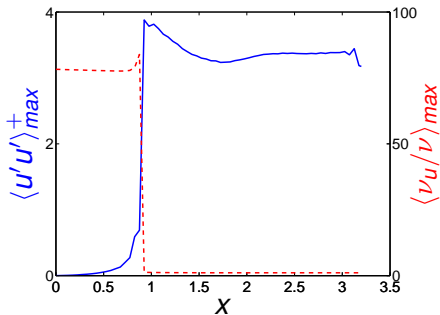
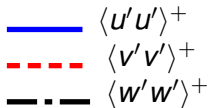
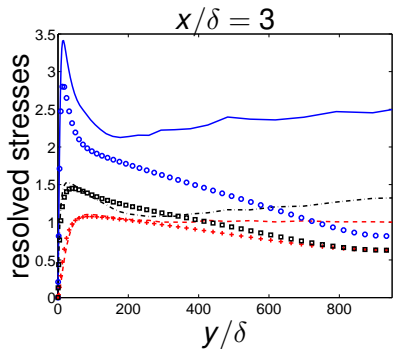
- For k_U & ε_U we prescribe “inlet” boundary conditions at the interface.
- First, the usual convective and diffusive fluxes at the interface are set to zero
- Next, new convective fluxes are added. Which “inlet” values should be used at the interface?
 - ▶ $k_{U,int} = f_k k_{RANS}(x = 0.5\delta)$, $\varepsilon_{U,int} = C_\mu^{3/4} k_{U,int}^{3/2} / \ell_{sgs}$, $\ell_{sgs} = C_s \Delta$,
 $\Delta = V^{1/3}$
 - ▶ Baseline $C_s = 0.07$; different C_s values are tested

CHANNEL FLOW: VELOCITY AND SHEAR STRESSES



— $x/\delta = 0.19$ - - - $x/\delta = 1.25$ - · - $x/\delta = 3$

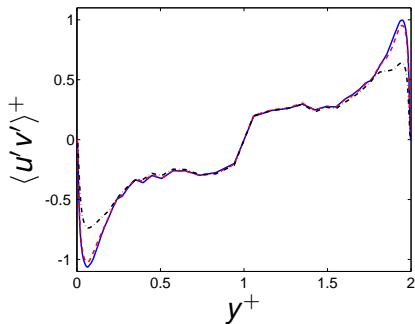
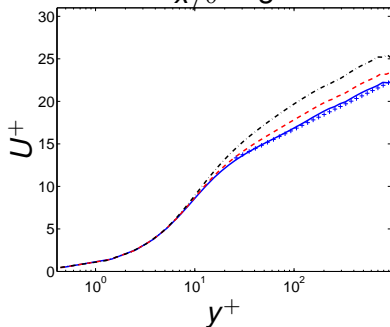
CHANNEL FLOW: STRESSES AND PEAK VALUES VS. x



CHANNEL FLOW: DIFFERENT C_S VALUE FOR $\varepsilon_{interface}$

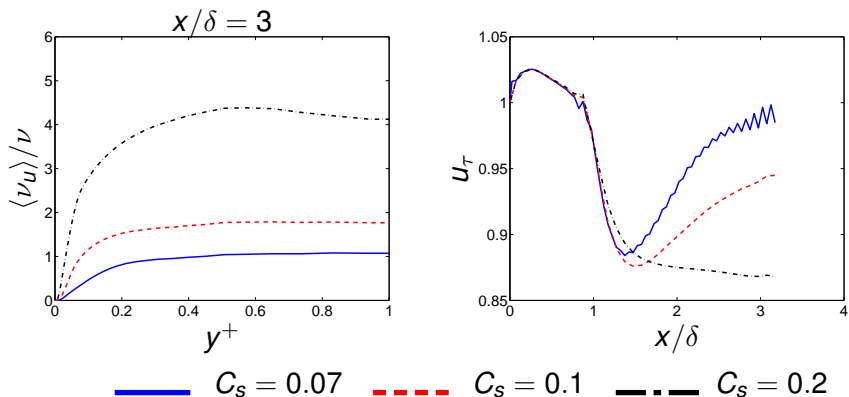
- $k_{u,int} = f_k k_{RANS}$
- $\varepsilon_{u,int} = C_\mu^{3/4} k_{u,int}^{3/2} / l_{sgs}$, $l_{sgs} = C_S \Delta$

$x/\delta = 3$

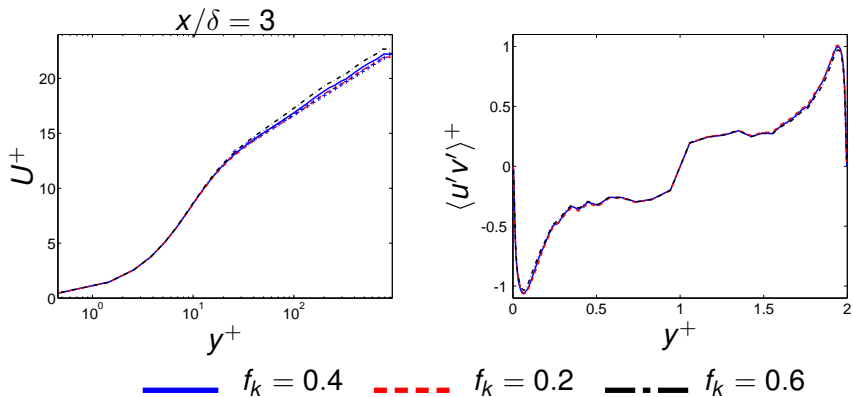


— $C_S = 0.07$ - - - $C_S = 0.1$ - . - $C_S = 0.2$

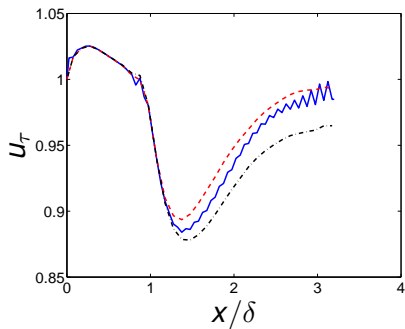
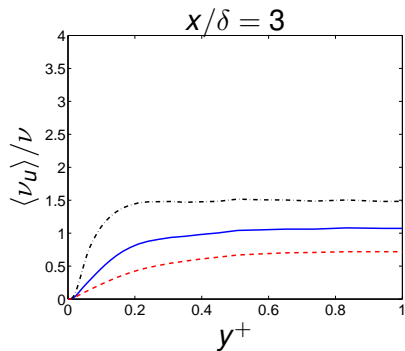
CHANNEL FLOW: DIFFERENT C_S VALUE FOR $\varepsilon_{interface}$



CHANNEL FLOW: DIFFERENT f_k VALUES

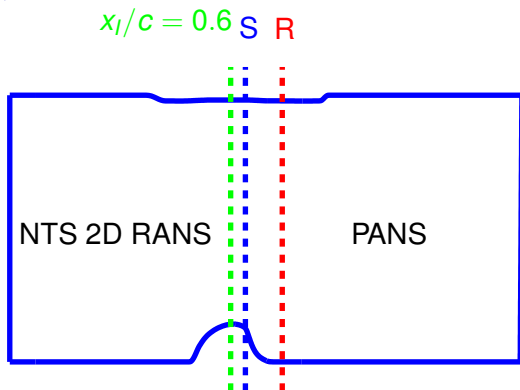


CHANNEL FLOW: DIFFERENT f_k VALUES



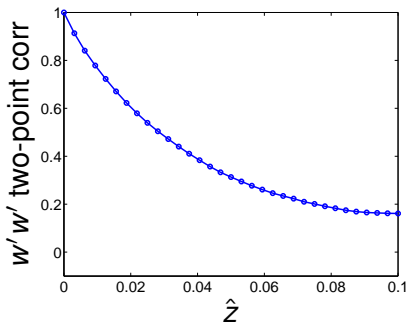
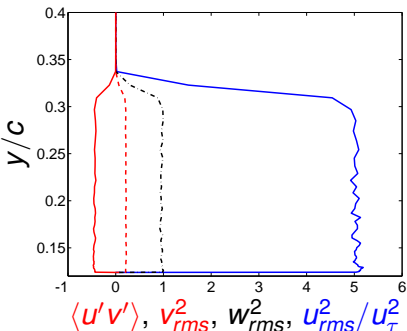
— $f_k = 0.4$ - - - $f_k = 0.2$ - . - $f_k = 0.6$

HUMP FLOW



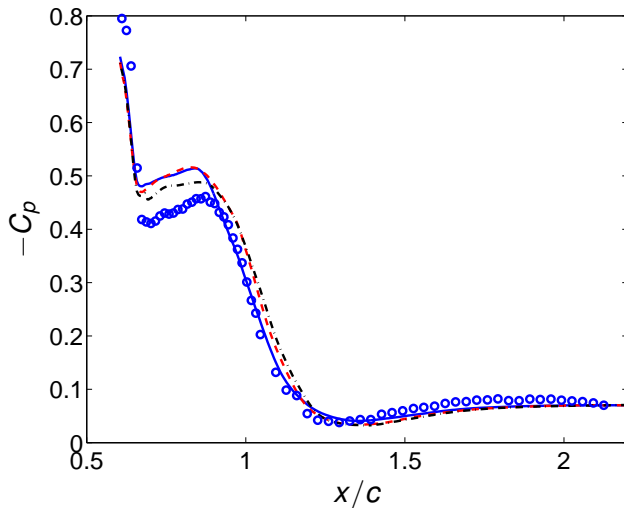
- **Inlet**, **Separation** $x_S/c = 0.65$; **reattachment** $x_R/c = 1.1$
- $Re_c = 936\,000 \frac{U_{ij}c}{\nu}$ ($U_{in} = c = \rho = 1, \nu = 1/Re_c$)
- $H/c = 0.91, h/c = 0.128, x/c = [0.6, 4.2]$
- Mesh: $312 \times 120 \times 64, Z_{max} = 0.2c$ (baseline)

BASELINE INLET FLUCTUATIONS



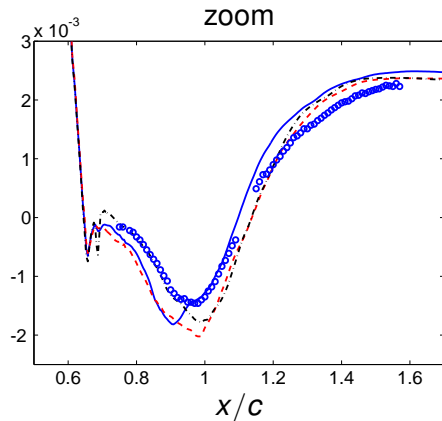
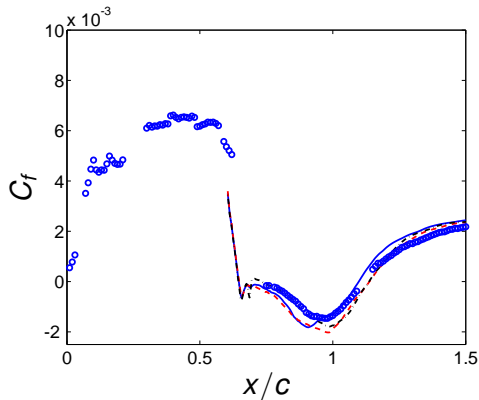
- Integral length scale $\mathcal{L} \simeq 0.04$ (see 2-p point correlation)
- Asymmetric time filter $(U')^m = a(U')^{m-1} + b(U')^m$ with $a = 0.954, b = (1 - a^2)^{1/2}$ gives a time integral scale $\mathcal{T} = 0.038$
- $\Delta t = 0.002$. 7500 + 7500 time steps (100 hours one core)
- Fluctuations multiplied by $f_{bl} = \max \{0.5 [1 - \tanh(y - y_{bl} - y_{wall})/b], 0.02\}$, $y_{bl} = 0.2$, $b = 0.01$.

PRESSURE: AMPLITUDES OF INLET FLUCT



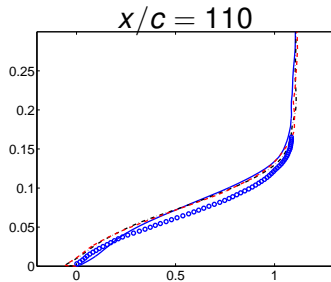
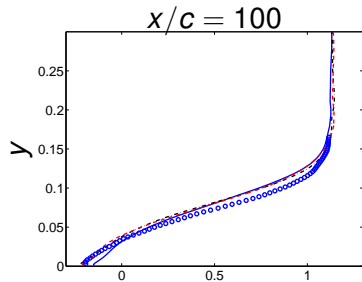
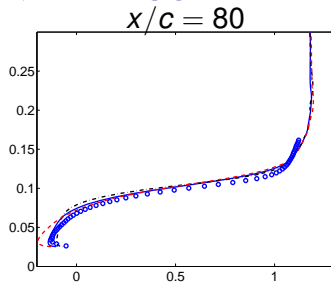
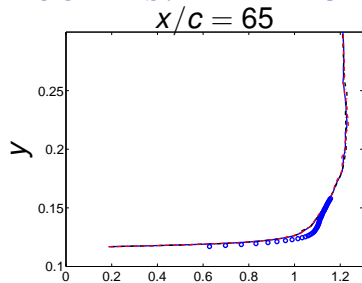
— baseline inlet fluct - - - 1.5× (baseline inlet fluct)
- . - 0.5× (baseline inlet fluct)

SKIN FRICTION: AMPLITUDES OF INLET FLUCT



— baseline inlet fluct - - - 1.5× (baseline inlet fluct)
- - - 0.5× (baseline inlet fluct)

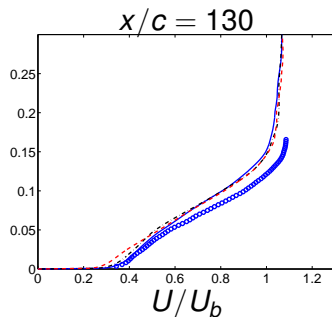
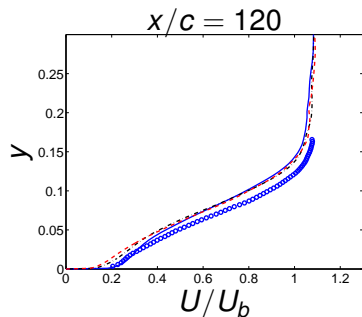
VELOCITIES: AMPLITUDES OF INLET FLUCT



— baseline **- - -** $1.5 \times$ (baseline) **- . -** $0.5 \times$ (baseline)

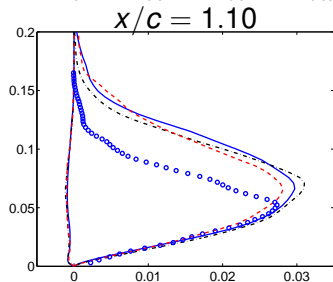
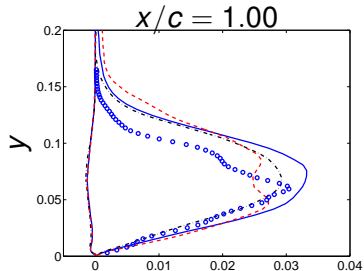
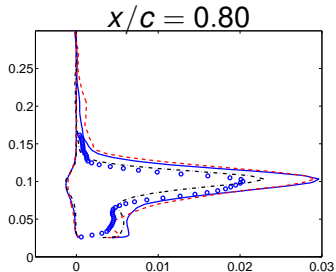
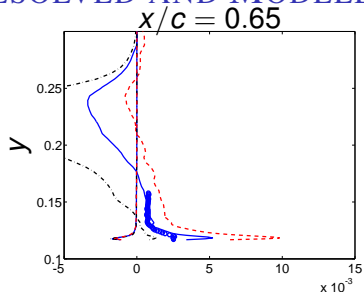
U/U_b U/U_b

VELOCITIES: AMPLITUDES OF INLET FLUCT



— baseline - - - 1.5× (baseline) - . - 0.5× (baseline)

RESOLVED AND MODELLED (< 0) SHEAR STRESSES



$\langle \tau_{12,u} \rangle, \langle -u'v' \rangle / U_b^2$

— baseline

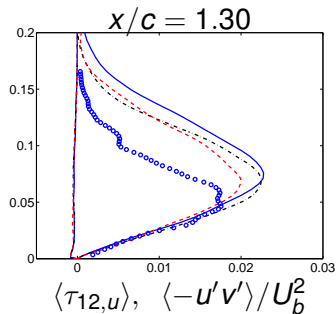
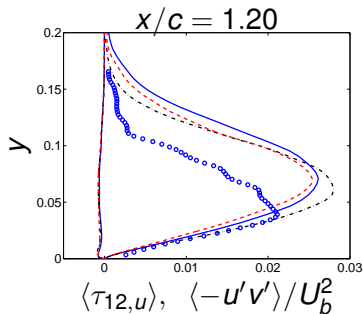
- - - $1.5 \times$ (baseline)

$\langle \tau_{12,u} \rangle, \langle -u'v' \rangle / U_b^2$

- - - $0.5 \times$ (baseline)

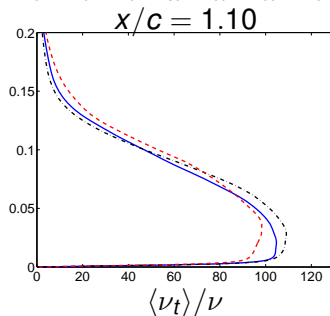
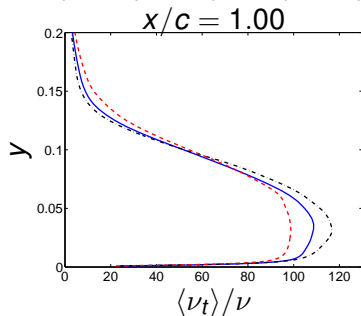
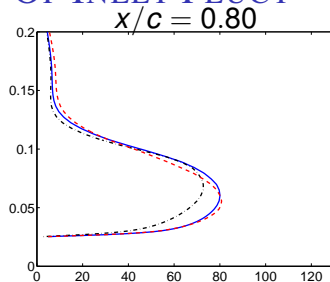
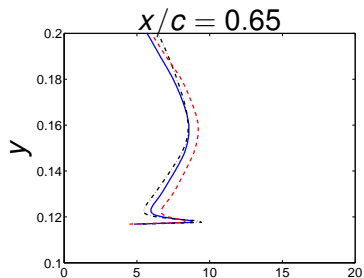
SHEAR STRESSES: AMPLITUDES OF INLET FLUCT

- Resolved and Modelled (< 0) Shear stresses



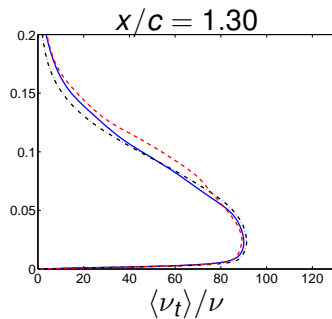
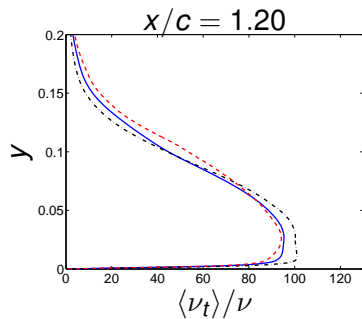
— baseline inlet fluct - - - 1.5× (baseline inlet fluct)
- . - 0.5× (baseline inlet fluct)

TURB VISCOSITY: AMPLITUDES OF INLET FLUCT



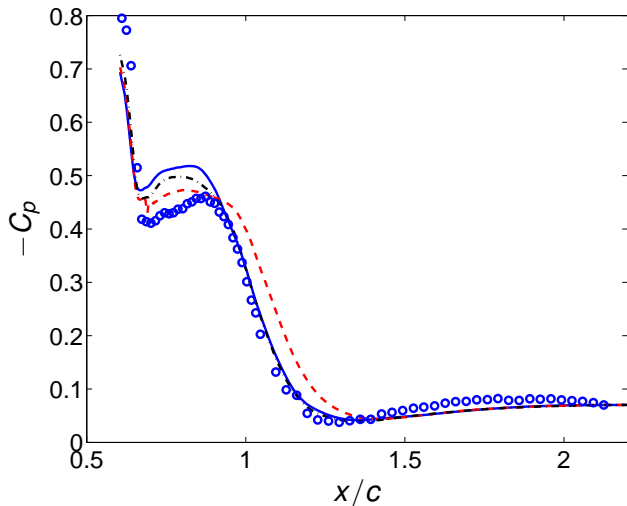
— baseline - - - $1.5 \times$ (baseline) - · - $0.5 \times$ (baseline)

TURB VISCOSITY: AMPLITUDES OF INLET FLUCT



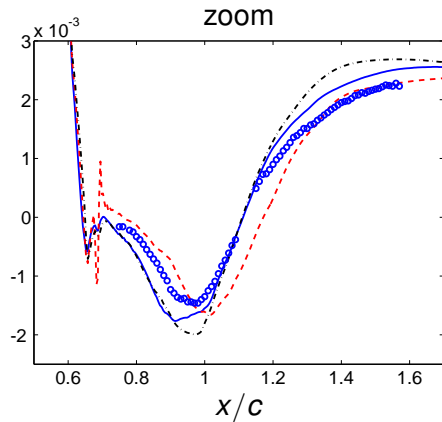
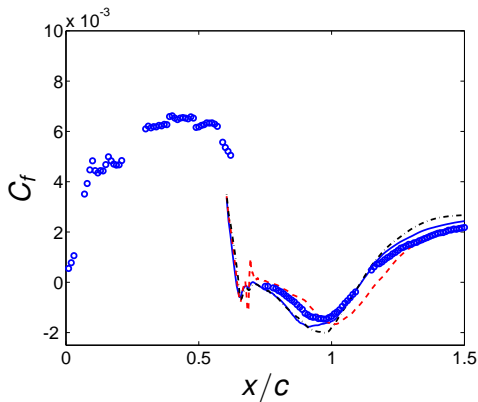
— baseline - - - 1.5× (baseline) - . - 0.5× (baseline)

PRESSURE: $f_k = 0.5$; NO INLET FLUCT; $N_k = 128$



— $N_k = 128$ - - - no inlet fluct - . - $f_k = 0.5$

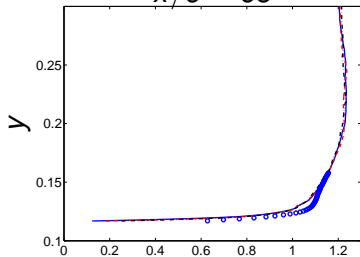
SKIN FRICTION: $f_k = 0.5$; NO INLET FLUCT; $N_k = 128$



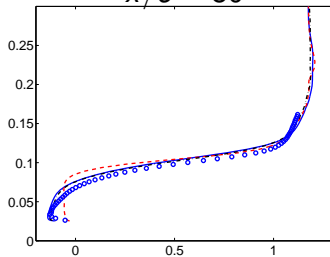
— $N_k = 128$ - - - no inlet fluct - . - $f_k = 0.5$

VELOCITIES: $f_k = 0.5$; NO INLET FLUCT; $N_k = 128$

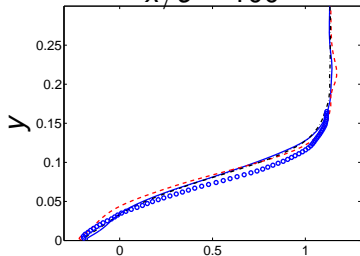
$x/c = 65$



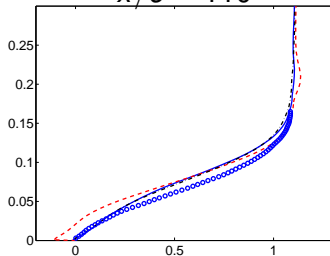
$x/c = 80$



$x/c = 100$



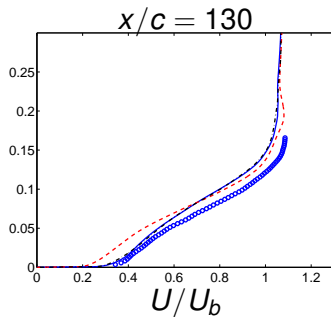
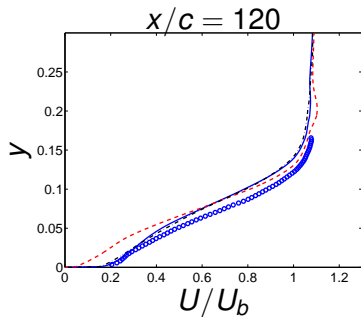
$x/c = 110$



— $N_k = 128$
- - - no inlet fluct

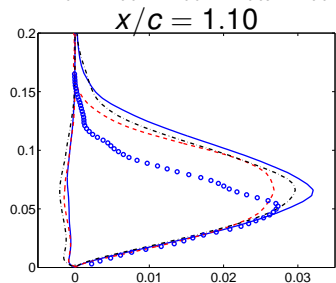
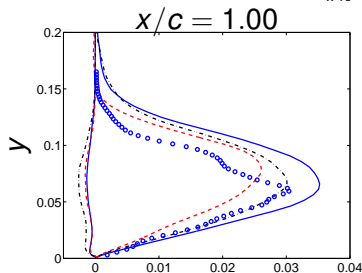
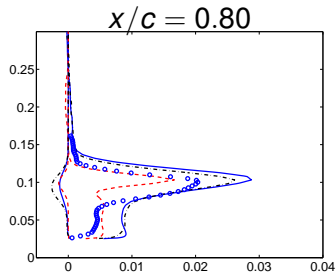
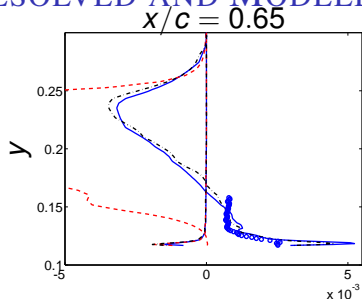
- · - · $f_k = 0.5$

VELOCITIES: $f_k = 0.5$; NO INLET FLUCT; $N_k = 128$



— $N_k = 128$ - - - no inlet fluct - . - $f_k = 0.5$

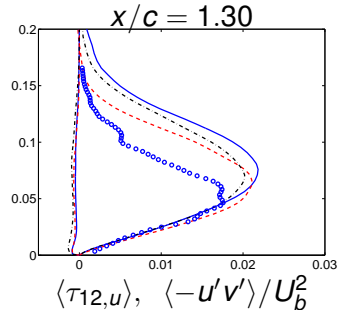
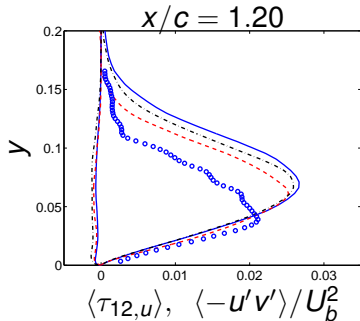
RESOLVED AND MODELLED (< 0) SHEAR STRESSES



$\langle \tau_{12,u} \rangle$, $\langle -u'v' \rangle / U_b^2$
— $N_k = 128$ - - - no inlet fluct - · - $f_k = 0.5$

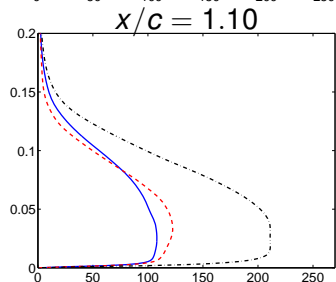
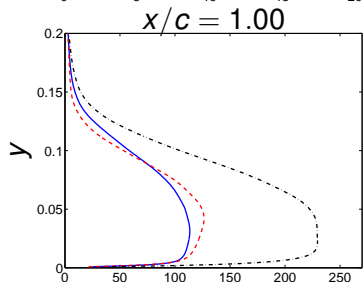
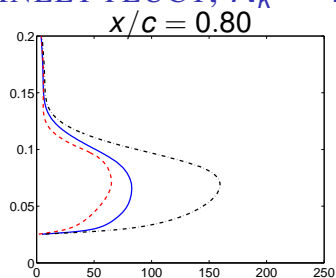
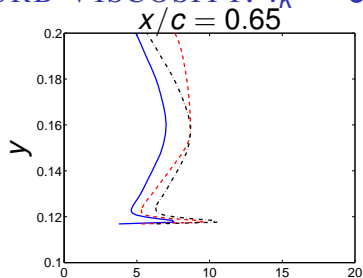
SHEAR STRESSES: $f_k = 0.5$; NO INLET FLUCT; $N_k = 128$

- Resolved and Modelled (< 0) Shear stresses



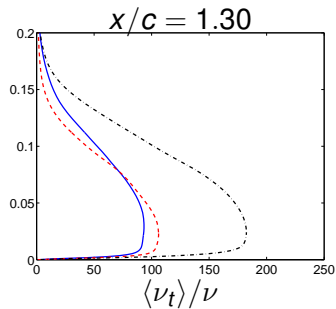
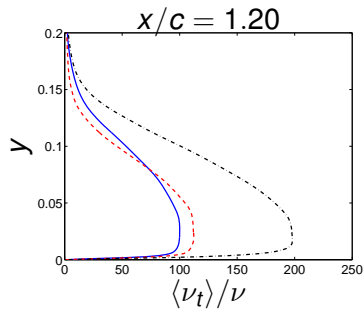
— $N_k = 128$ - - - no inlet fluct - . - $f_k = 0.5$

TURB VISCOSITY: $f_k = 0.5$; NO INLET FLUCT; $N_k = 128$



— $N_k = 128$
 - - - no inlet fluct
 - · - · $f_k = 0.5$

TURB VISCOSITY: $f_k = 0.5$; NO INLET FLUCT; $N_k = 128$



— $N_k = 128$ - - - no inlet fluct - . - $f_k = 0.5$

CONCLUDING REMARKS

- LRN PANS has been shown to **work well** as an embedded LES method
- Channel flow: At **two δ** downstream the interface, the **resolved turbulence** in good agreement with DNS data and the wall friction velocity has reached **99%** of its fully developed value.
- Channel flow: The treatment of the modelled **k_u and ε_u** across the interface is important.
- LRN PANS predicts the hump flow **well** but the **recover rate** slightly too slow
- Hump flow: large **(small)** inlet fluctuations gives a smaller **(larger)** recirculation

PANS: CONCLUDING REMARKS

- Embedded LES with $k - \varepsilon$ PANS and Synthetic b.c.

PANS: CONCLUDING REMARKS

- Embedded LES with $k - \varepsilon$ PANS and Synthetic b.c.
- Channel flow

PANS: CONCLUDING REMARKS

- Embedded LES with $k - \varepsilon$ PANS and Synthetic b.c.
- Channel flow
 - ▶ **Isotropic** fluctuations work **well** for channel flow

PANS: CONCLUDING REMARKS

- Embedded LES with $k - \varepsilon$ PANS and Synthetic b.c.
- Channel flow
 - ▶ **Isotropic** fluctuations work **well** for channel flow
 - ▶ **Strong** dependence on interface k_u & ε_u values

PANS: CONCLUDING REMARKS

- Embedded LES with $k - \varepsilon$ PANS and Synthetic b.c.
- Channel flow
 - ▶ **Isotropic** fluctuations work **well** for channel flow
 - ▶ **Strong** dependence on interface k_u & ε_u values
 - ▶ **No strong** dependence on amplitude, L or \mathcal{T} of fluctuations

PANS: CONCLUDING REMARKS CONT'D

- Hump flow

PANS: CONCLUDING REMARKS CONT'D

- Hump flow
 - ▶ PANS & synthetic inlet b.c. with f_k everywhere gives good results except C_f (error > 50%)

PANS: CONCLUDING REMARKS CONT'D

- Hump flow

- ▶ PANS & synthetic inlet b.c. with f_k everywhere gives good results except C_f (error > 50%)
- ▶ With embedded **isotropic** fluctuations, interface must be located far upstream

PANS: CONCLUDING REMARKS CONT'D

- Hump flow

- ▶ PANS & synthetic inlet b.c. with f_k everywhere gives good results except C_f (error > 50%)
- ▶ With embedded **isotropic** fluctuations, interface must be located far upstream
- ▶ With embedded **anisotropic** fluctuations, good results are obtained, still poor C_f

PANS: CONCLUDING REMARKS CONT'D

- Hump flow

- ▶ PANS & synthetic inlet b.c. with f_k everywhere gives good results except C_f (error > 50%)
- ▶ With embedded **isotropic** fluctuations, interface must be located far upstream
- ▶ With embedded **anisotropic** fluctuations, good results are obtained, still poor C_f
- ▶ **On-going** work ...

Large Eddy Simulation of Heat Transfer in Boundary layer and Backstep Flow Using PANS [6]

Lars Davidson

THMT-12, Palermo, Sept 2012

PANS LOW REYNOLDS NUMBER MODEL [17]

$$\frac{\partial k_u}{\partial t} + \frac{\partial(k_u U_j)}{\partial x_j} = \frac{\partial}{\partial x_j} \left[\left(\nu + \frac{\nu_u}{\sigma_{ku}} \right) \frac{\partial k_u}{\partial x_j} \right] + (P_u - \varepsilon_u)$$

$$\frac{\partial \varepsilon_u}{\partial t} + \frac{\partial(\varepsilon_u U_j)}{\partial x_j} = \frac{\partial}{\partial x_j} \left[\left(\nu + \frac{\nu_u}{\sigma_{\varepsilon u}} \right) \frac{\partial \varepsilon_u}{\partial x_j} \right] + C_{\varepsilon 1} P_u \frac{\varepsilon_u}{k_u} - C_{\varepsilon 2}^* \frac{\varepsilon_u^2}{k_u}$$

$$\nu_u = C_\mu f_\mu \frac{k_u^2}{\varepsilon_u}, C_{\varepsilon 2}^* = C_{\varepsilon 1} + \frac{f_k}{f_\varepsilon} (C_{\varepsilon 2} f_2 - C_{\varepsilon 1}), \sigma_{ku} \equiv \sigma_k \frac{f_k^2}{f_\varepsilon}, \sigma_{\varepsilon u} \equiv \sigma_\varepsilon \frac{f_k^2}{f_\varepsilon}$$

$C_{\varepsilon 1}$, $C_{\varepsilon 2}$, σ_k , σ_ε and C_μ same values as [1]. $f_\varepsilon = 1$. f_2 and f_μ read

$$f_2 = \left[1 - \exp\left(-\frac{y^*}{3.1}\right) \right]^2 \left\{ 1 - 0.3 \exp\left[-\left(\frac{R_t}{6.5}\right)^2\right] \right\}$$

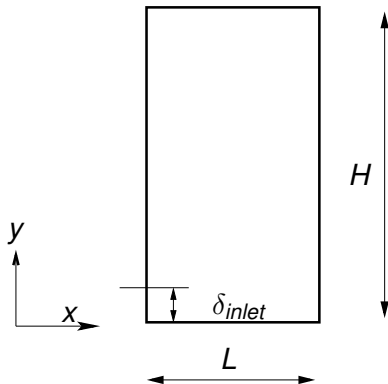
$$f_\mu = \left[1 - \exp\left(-\frac{y^*}{14}\right) \right]^2 \left\{ 1 + \frac{5}{R_t^{3/4}} \exp\left[-\left(\frac{R_t}{200}\right)^2\right] \right\}$$

- Baseline model: $f_k = 0.4$.

NUMERICAL METHOD

- Incompressible finite volume method
- Pressure-velocity coupling treated with fractional step
- Differencing scheme for momentum eqns:
 - ▶ 95% 2^{nd} order **central** and 5% 2^{nd} order **upwind** differencing scheme (baseline) **OR**
 - ▶ 100% 2^{nd} order **central** differencing
- Hybrid **1st order upwind**/ 2^{nd} order central scheme k & ε eqns.
- **2^{nd} -order** Crank-Nicholson for time discretization

BOUNDARY LAYER FLOW: DOMAIN

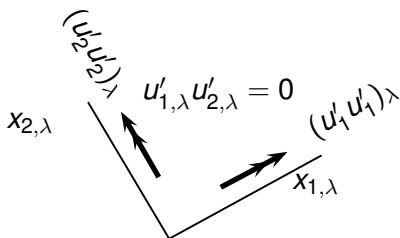


- Inlet: $\delta_{inlet} = 1$ (covered by 45 cells), $Re_{\theta} = 3600$, $U_{in} = \rho = 1$.
Stretching 1.12 up to $y/\delta \simeq 1$.
- Domain: $L/\delta_{in} = 3.2$, $H/\delta_{in} = 15.6$, $Z_{max} = 1.5\delta_{in}$
- Resolution: $\Delta z_{in}^+ \simeq 27$, $\Delta x_{in}^+ \simeq 54$
- Grid: $66 \times 96 \times 64$ (x, y, z)

ANISOTROPIC SYNTHETIC FLUCTUATIONS: I [3, 2, 8]

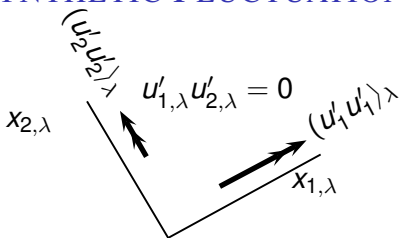
- Prescribe an homogeneous Reynolds tensor, $\overline{u_i u_j}$ (here from DNS)
-
-

ANISOTROPIC SYNTHETIC FLUCTUATIONS: I [3, 2, 8]



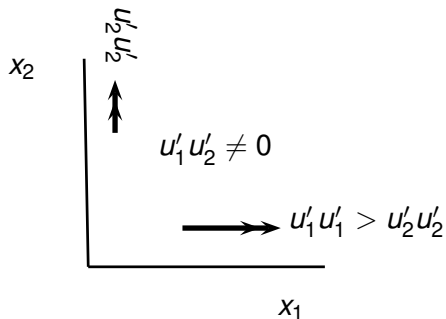
- Prescribe an homogeneous Reynolds tensor, $\overline{u_i u_j}$ (here from DNS)
- isotropic fluctuations in principal directions, $(u'_1 u'_1)_\lambda = (u'_2 u'_2)_\lambda$, $u'_{1,\lambda} u'_{2,\lambda} = 0$
-

ANISOTROPIC SYNTHETIC FLUCTUATIONS: I [3, 2, 8]



- Prescribe an homogeneous Reynolds tensor, $\overline{u_i u_j}$ (here from DNS)
- isotropic fluctuations in principal directions, $(u'_1 u'_1)_\lambda = (u'_2 u'_2)_\lambda$,
 $u'_{1,\lambda} u'_{2,\lambda} = 0$
- re-scale the normal components, $(u'_1 u'_1)_\lambda > (u'_2 u'_2)_\lambda$,
 $u'_{1,\lambda} u'_{2,\lambda} = 0$

ANISOTROPIC SYNTHETIC FLUCTUATIONS: II

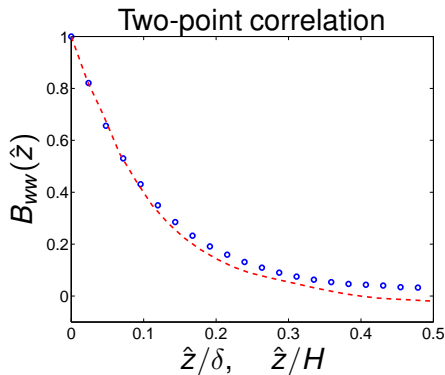
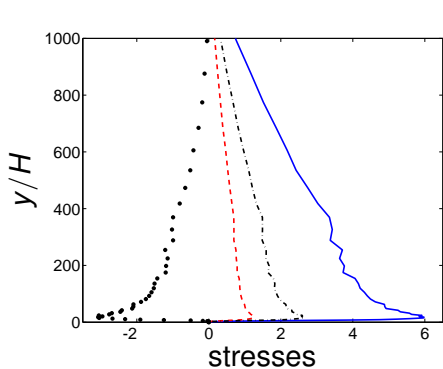


- Transform from $(x_{1,\lambda}, x_{2,\lambda})$ to (x_1, x_2)
- $\frac{u_1'^2}{u_2'^2} = 23, \frac{u_1'^2}{u_3'^2} = 5$ from $(u_1' u_1')_{peak}$ in DNS channel flow, $Re_\tau = 500$

INLET CONDITIONS FOR k_u AND ε_u AS IN [10]

- A pre-cursor RANS simulation using the AKN model (i.e. PANS with $f_k = 1$) is carried out. At $Re_\theta = 3600$, U_{RANS} , V_{RANS} , k_{RANS} are taken.
- $\bar{u}_{in} = U_{RANS} + u'_{synt}$, $\bar{v}_{in} = V_{RANS} + v'_{synt}$, $\bar{w}_{in} = w'_{synt}$
- Anisotropic synthetic fluctuations are used. The fluctuations are scaled with $k_u/k_{u,max}$.
- $k_{u,in} = f_k k_{RANS}$, $\varepsilon_{u,in} = C_\mu^{3/4} k_{u,in}^{3/2} / \ell_{sgs}$, $\ell_{sgs} = C_s \Delta$, $\Delta = V^{1/3}$,
 $C_s = 0.05$

INLET TURB. FLUCTUATION, TWO-POINT CORRELATIONS



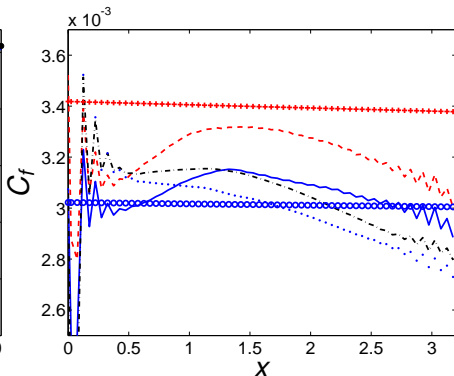
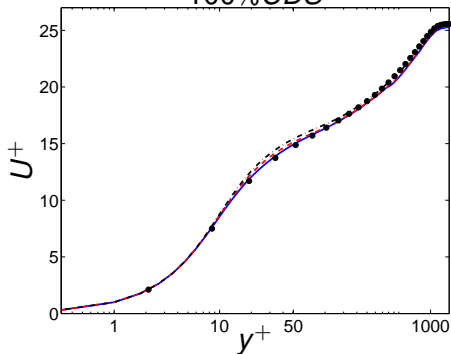
— u_{rms}^{+2}
- - - w_{rms}^{+2}
. . . $\langle u'v' \rangle^+$

- - - v_{rms}^{+2}

○: inlet; - - - $x = 3\delta_{in}$

BOUNDARY LAYER: VELOCITY AND SKIN FRICTION

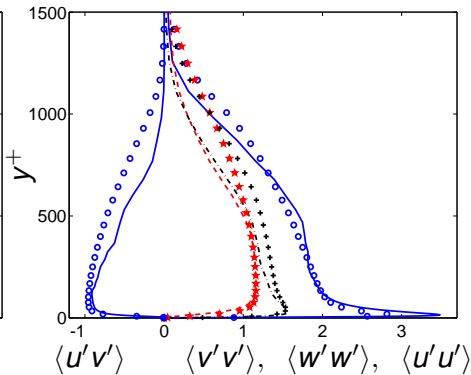
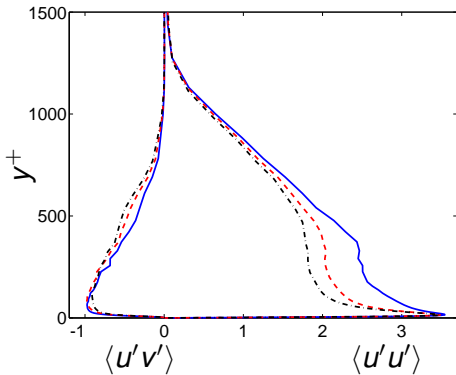
100% CDS



— $x = \delta_{in}$; - - - $x = 2\delta_{in}$;
- . - $x = 3\delta_{in}$; ■: DNS [21]

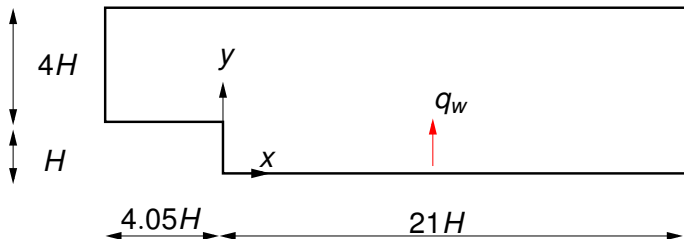
— 100% CDS; - - - 100% CDS, U_{in} from AKN; - . - 25% larger inlet fluct.; ⋯ 25% larger inlet fluct., $C_s = 0.07$; markers: $0.37 (\log_{10} Re_x)^{-2.584}$ (+: AKN; ○: DNS)

REYNOLDS STRESSES



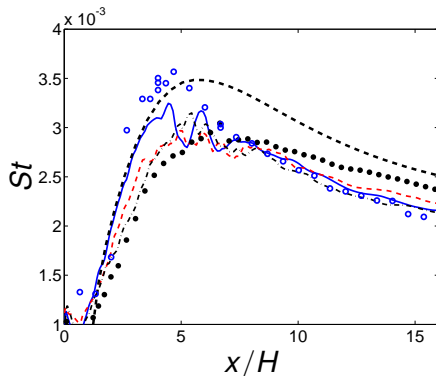
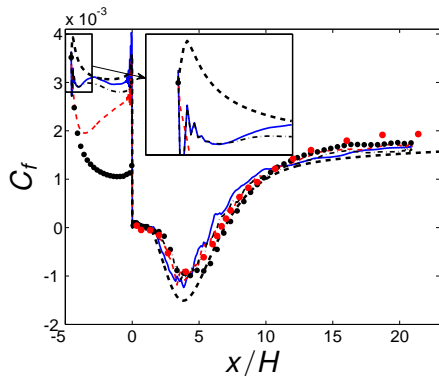
— $x = \delta_{in}$; - - - $x = 2\delta_{in}$; - · - · - $x = 3\delta_{in}$; Markers: DNS [21]

BACKWARD FACING STEP: DOMAIN



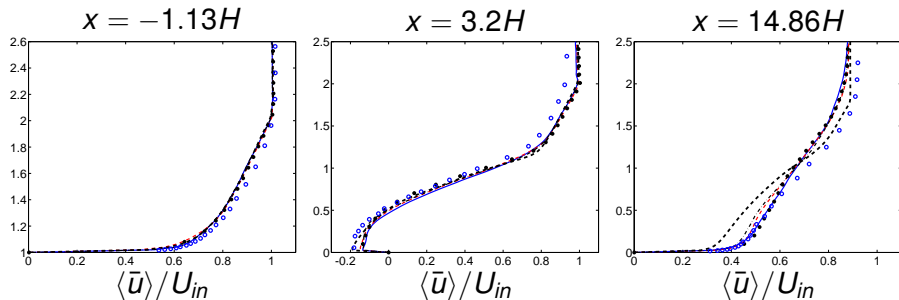
- $Re_H = 28\,000$ Experiments by Vogel & Eaton [26]
- Mean inlet profiles from RANS (same as in boundary layer)
- Grid: 336×120 in $x \times y$ plane. $Z_{max} = 1.6H$, $N_k = 64$, $\Delta z_{in}^+ = 31$.
- Anisotropic synthetic fluctuations, u' , v' , w' (same as for boundary layer flow); no fluctuations for t'
- Constant heat flux, q_w , on lower wall.

BACKSTEP FLOW. SKIN FRICTION AND STANTON NUMBER



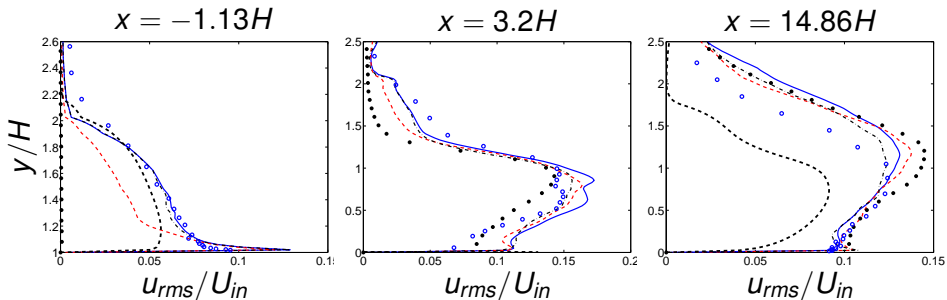
— PANS; - - - PANS, 50% smaller inlet fluctuations;
- · - WALE; ●: PANS, no inlet fluctuations; - - - : 2D RANS; ○, ●: experiments [26].

BACKSTEP FLOW: VELOCITIES.



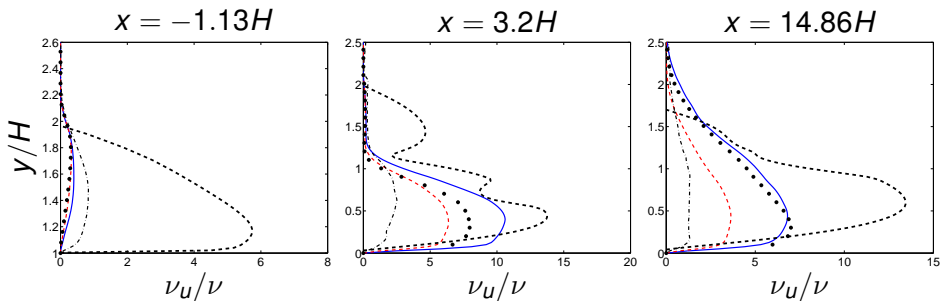
- PANS; - - - PANS, 50% smaller inlet fluctuations;
- . - . WALE;
●: PANS, no inlet fluctuations; - - - : 2D RANS; ○: experiments [26].

BACKSTEP FLOW: RESOLVED STREAMWISE STRESS.



- PANS; - - - PANS, 50% smaller inlet fluctuations;
- - - WALE;
●: PANS, no inlet fluctuations; - - - : 2D RANS; ○: experiments [26].

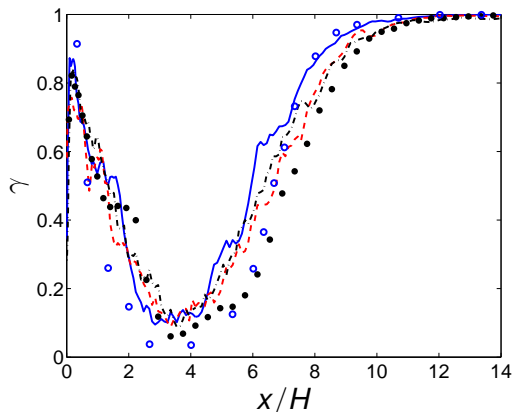
BACKSTEP FLOW: TURBULENT VISCOSITIES.



- PANS; - - - PANS, 50% smaller inlet fluctuations;
- - - WALE;
●: PANS, no inlet fluctuations; - - - : 2D RANS/10;

FORWARD/BACKWARD FLOW

- Fraction of time, γ , when the flow along the bottom wall is in the downstream direction.

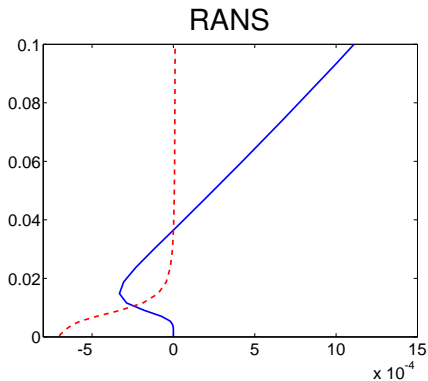
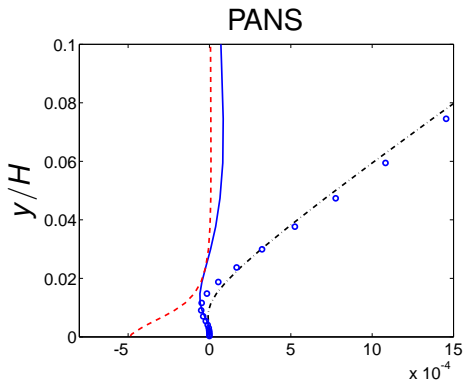


— PANS; - - - PANS, 50% smaller inlet fluctuations;

- - - WALE;

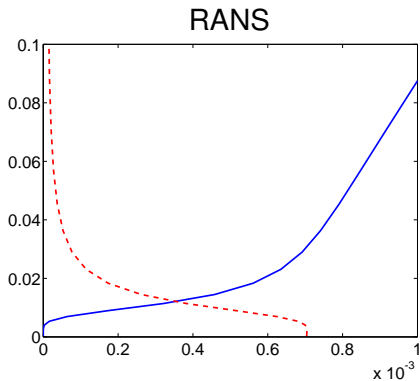
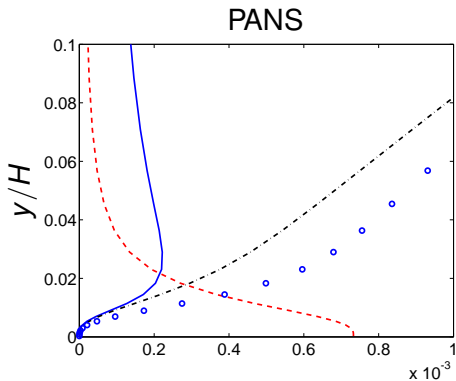
●: PANS, no inlet fluctuations; ○: experiments [26].

SHEAR STRESSES. $x = 3.2H$



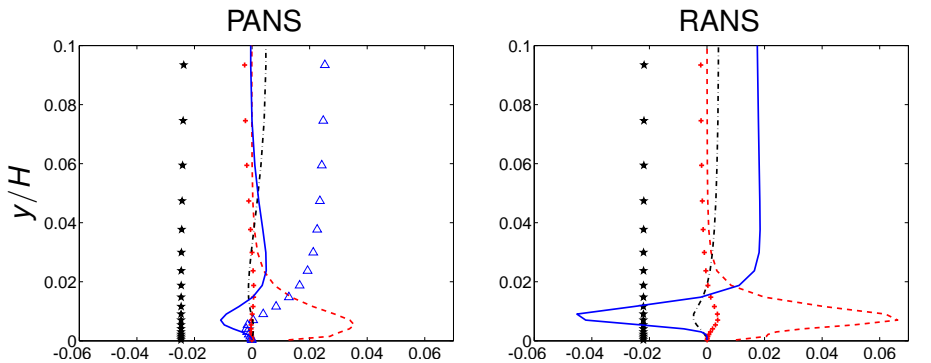
— $2\langle \nu_t \bar{s}_{12} \rangle$;
 - - - $\nu \frac{\partial \langle \bar{u} \rangle}{\partial y}$;
 - · - $-\langle \langle u'v' \rangle \rangle$;
 ○ $2\langle \nu_t \bar{s}_{12} \rangle - \langle \langle u'v' \rangle \rangle$.

SHEAR STRESSES. $x = 14.86$



— $2\langle \nu_t \bar{s}_{12} \rangle$;
 - - - $\nu \frac{\partial \langle \bar{u} \rangle}{\partial y}$;
 - · - $-\langle \langle u'v' \rangle \rangle$;
 ○ $2\langle \nu_t \bar{s}_{12} \rangle - \langle \langle u'v' \rangle \rangle$.

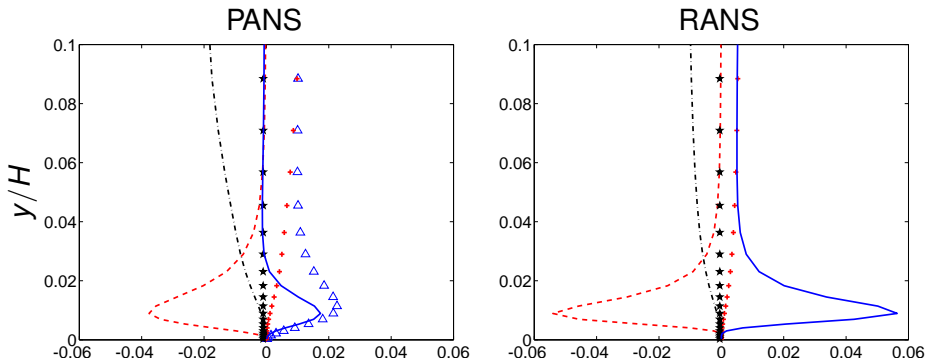
TERMS IN THE $\langle \bar{u} \rangle$ EQUATION. $x = 3.2H$



— $\frac{\partial}{\partial y} (2\langle \nu_t \bar{s}_{12} \rangle)$; - - - $\nu \frac{\partial^2 \langle \bar{u} \rangle}{\partial y^2}$; - · - · $-\frac{\partial \langle \bar{u} \rangle \langle \bar{u} \rangle}{\partial x}$; + $-\frac{\partial \langle \bar{u} \rangle \langle \bar{v} \rangle}{\partial y}$;

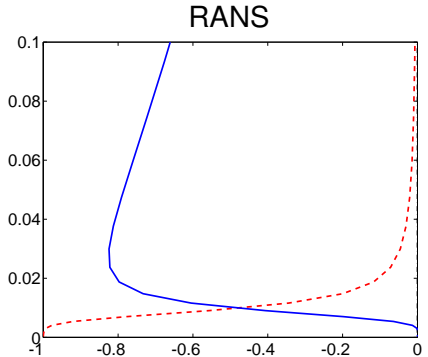
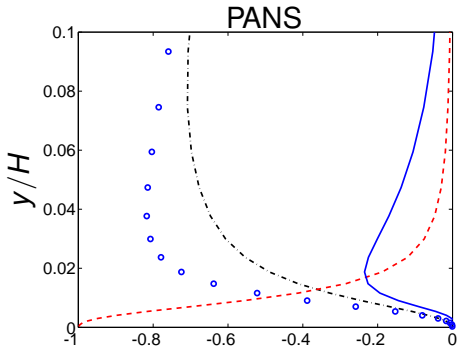
*: $-\frac{\partial \langle \bar{p} \rangle}{\partial x}$, △: $-\frac{\partial \langle \langle u'v' \rangle \rangle}{\partial y}$.

TERMS IN THE $\langle \bar{u} \rangle$ EQUATION. $x = 14.86H$



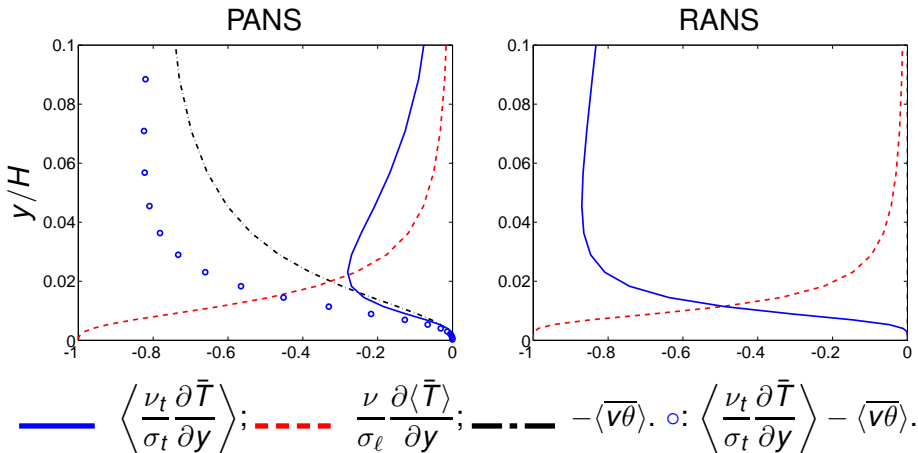
— $\frac{\partial}{\partial y} (2\langle \nu_t \bar{s}_{12} \rangle)$; - - - $\nu \frac{\partial^2 \langle \bar{u} \rangle}{\partial y^2}$; - · - $-\frac{\partial \langle \bar{u} \rangle \langle \bar{u} \rangle}{\partial x}$; + $-\frac{\partial \langle \bar{u} \rangle \langle \bar{v} \rangle}{\partial y}$;
*: $-\frac{\partial \langle \bar{p} \rangle}{\partial x}$, △: $-\frac{\partial \langle \langle u'v' \rangle \rangle}{\partial y}$.

HEAT FLUXES. $x = 3.2H$

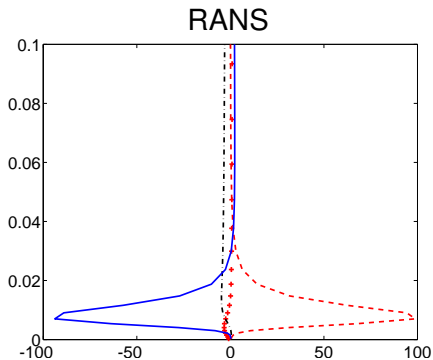
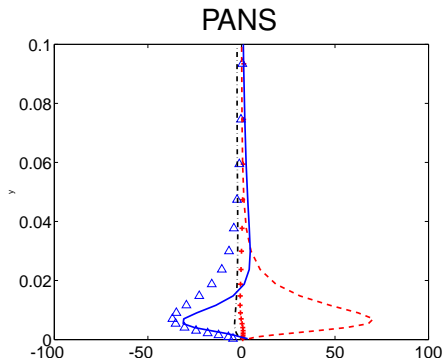


— $\left\langle \frac{\nu_t}{\sigma_t} \frac{\partial \bar{T}}{\partial y} \right\rangle$;
 - - - $\frac{\nu}{\sigma_l} \frac{\partial \langle \bar{T} \rangle}{\partial y}$;
 - · - · $-\langle \bar{v}\theta \rangle$.
 ○: $\left\langle \frac{\nu_t}{\sigma_t} \frac{\partial \bar{T}}{\partial y} \right\rangle - \langle \bar{v}\theta \rangle$.

HEAT FLUXES. $x = 14.86H$

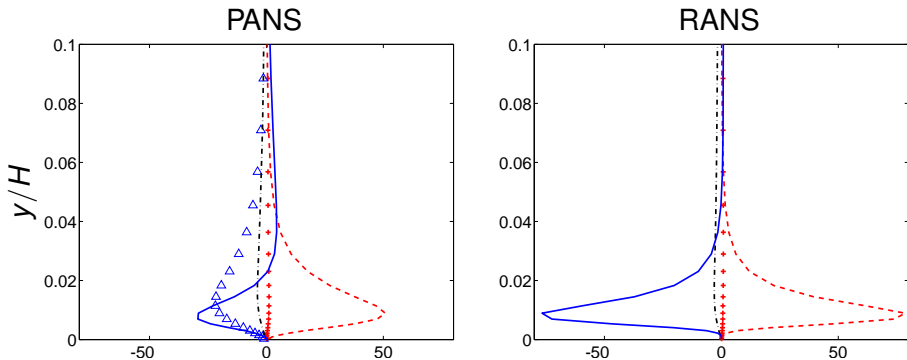


TERMS IN THE $\langle \bar{T} \rangle$ EQUATION. $x = 3.2H$



$$\begin{aligned}
 & \text{---} \frac{\partial}{\partial y} \left(\frac{\nu_t}{\sigma_t} \frac{\partial \langle \bar{T} \rangle}{\partial y} \right); \quad \text{---} \frac{\nu}{\sigma_l} \frac{\partial^2 \langle \bar{T} \rangle}{\partial y^2}; \quad \text{---} - \frac{\partial \langle \bar{u} \rangle \langle \bar{T} \rangle}{\partial x}; \quad +: \\
 & - \frac{\partial \langle \bar{v} \rangle \langle \bar{T} \rangle}{\partial y}; \quad \triangle: - \frac{\partial \langle \bar{v} \theta \rangle}{\partial y}.
 \end{aligned}$$

TERMS IN THE $\langle \bar{T} \rangle$ EQUATION. $x = 14.86H$



$$\begin{aligned}
 & \text{---} \frac{\partial}{\partial y} \left(\frac{\nu_t}{\sigma_t} \frac{\partial \langle \bar{T} \rangle}{\partial y} \right); \quad \text{---} \frac{\nu}{\sigma_l} \frac{\partial^2 \langle \bar{T} \rangle}{\partial y^2}; \quad \text{---} \frac{\partial \langle \bar{u} \rangle \langle \bar{T} \rangle}{\partial x}; \quad +: \\
 & - \frac{\partial \langle \bar{v} \rangle \langle \bar{T} \rangle}{\partial y}; \quad \triangle: - \frac{\partial \langle \bar{v} \theta \rangle}{\partial y}.
 \end{aligned}$$

CONCLUDING REMARKS

- Developing boundary layer
 - ▶ Synthetic fluctuations give **fully developed conditions** after a **couple** of boundary layer thicknesses
 - ▶ 5% upwinding dampens resolved fluctuations; can be compensated by 25% larger inlet fluctuations
- Backstep flow
 - ▶ Very **good** agreement with experiments
 - ▶ 2D RANS predicts turbulent diffusion surprisingly well
 - ▶ Synthetic inlet fluctuations give an improved Stanton number; otherwise small effect in the recirculation region
 - ▶ LRN PANS and WALE equally good
 - ▶ 5% upwinding has a negligible effect in the recirculation region

REFERENCES I

- [1] ABE, K., KONDOH, T., AND NAGANO, Y.
A new turbulence model for predicting fluid flow and heat transfer in separating and reattaching flows - 1. Flow field calculations.
Int. J. Heat Mass Transfer 37 (1994), 139–151.
- [2] BILLSON, M.
Computational Techniques for Turbulence Generated Noise.
PhD thesis, Dept. of Thermo and Fluid Dynamics, Chalmers University of Technology, Göteborg, Sweden, 2004.
- [3] BILLSON, M., ERIKSSON, L.-E., AND DAVIDSON, L.
Modeling of synthetic anisotropic turbulence and its sound emission.
The 10th AIAA/CEAS Aeroacoustics Conference, AIAA 2004-2857, Manchester, United Kindom, 2004.

REFERENCES II

- [4] DAVIDSON, L.
Large eddy simulations: how to evaluate resolution.
International Journal of Heat and Fluid Flow 30, 5 (2009),
1016–1025.
- [5] DAVIDSON, L.
How to estimate the resolution of an LES of recirculating flow.
In *ERCOFTAC* (2010), M. V. Salvetti, B. Geurts, J. Meyers, and
P. Sagaut, Eds., vol. 16 of *Quality and Reliability of Large-Eddy
Simulations II*, Springer, pp. 269–286.
- [6] DAVIDSON, L.
Large eddy simulation of heat transfer in boundary layer and
backstep flow using pans (to be presented).
In *Turbulence, Heat and Mass Transfer, THMT-12* (Palermo,
Sicily/Italy, 2012).

REFERENCES III

- [7] DAVIDSON, L.
A new approach of zonal hybrid RANS-LES based on a two-equation $k - \varepsilon$ model.
In ETMM9: International ERCOFTAC Symposium on Turbulence Modelling and Measurements (Thessaloniki, Greece, 2012).
- [8] DAVIDSON, L., AND BILLSON, M.
Hybrid LES/RANS using synthesized turbulence for forcing at the interface.
International Journal of Heat and Fluid Flow 27, 6 (2006), 1028–1042.
- [9] DAVIDSON, L., AND DAHLSTRÖM, S.
Hybrid LES-RANS: An approach to make LES applicable at high Reynolds number.
International Journal of Computational Fluid Dynamics 19, 6 (2005), 415–427.

REFERENCES IV

- [10] DAVIDSON, L., AND PENG, S.-H.
Emdedded LES with PANS.
In 6th AIAA Theoretical Fluid Mechanics Conference, AIAA paper 2011-3108 (27-30 June, Honolulu, Hawaii, 2011).
- [11] DAVIDSON, L., AND PENG, S.-H.
Embedded LES using PANS applied to channel flow and hump flow (to appear).
AIAA Journal (2013).
- [12] HEMIDA, H., AND KRAJNOVIĆ, S.
LES study of the impact of the wake structures on the aerodynamics of a simplified ICE2 train subjected to a side wind.
In Fourth International Conference on Computational Fluid Dynamics (ICCFD4) (10-14 July, Ghent, Belgium, 2006).

REFERENCES V

- [13] HINZE, J.
Turbulence, 2nd ed.
McGraw-Hill, New York, 1975.
- [14] KRAJNOVIĆ, S., AND DAVIDSON, L.
Large eddy simulation of the flow around a bluff body.
AIAA Journal 40, 5 (2002), 927–936.
- [15] KRAJNOVIĆ, S., AND DAVIDSON, L.
Numerical study of the flow around the bus-shaped body.
Journal of Fluids Engineering 125 (2003), 500–509.
- [16] KRAJNOVIĆ, S., AND DAVIDSON, L.
Flow around a simplified car. part II: Understanding the flow.
Journal of Fluids Engineering 127, 5 (2005), 919–928.

REFERENCES VI

- [17] MA, J., PENG, S.-H., DAVIDSON, L., AND WANG, F.
A low Reynolds number variant of Partially-Averaged Navier-Stokes model for turbulence.
International Journal of Heat and Fluid Flow 32 (2011), 652–669.
- [18] MENTER, F.
Two-equation eddy-viscosity turbulence models for engineering applications.
AIAA Journal 32 (1994), 1598–1605.
- [19] MENTER, F., KUNTZ, M., AND LANGTRY, R.
Ten years of industrial experience of the SST turbulence model.
In *Turbulence Heat and Mass Transfer 4* (New York, Wallingford (UK), 2003), K. Hanjalić, Y. Nagano, and M. Tummers, Eds., begell house, inc., pp. 624–632.

REFERENCES VII

- [20] POPE, S.
Turbulent Flow.
Cambridge University Press, Cambridge, UK, 2001.
- [21] SCHLATTER, P., AND ORLU, R.
Assessment of direct numerical simulation data of turbulent boundary layers.
Journal of Fluid Mechanics 659 (2010), 116–126.
- [22] SCHLICHTING, H.
Boundary-Layer Theory, 7 ed.
McGraw-Hill, New York, 1979.
- [23] SMAGORINSKY, J.
General circulation experiments with the primitive equations.
Monthly Weather Review 91 (1963), 99–165.

REFERENCES VIII

- [24] SPALART, P., JOU, W.-H., STRELETS, M., AND ALLMARAS, S.
Comments on the feasibility of LES for wings and on a hybrid RANS/LES approach.
In Advances in LES/DNS, First Int. conf. on DNS/LES (Louisiana Tech University, 1997), C. Liu and Z. Liu, Eds., Greyden Press.
- [25] STRELETS, M.
Detached eddy simulation of massively separated flows.
AIAA paper 2001–0879, Reno, NV, 2001.
- [26] VOGEL, J., AND EATON, J.
Combined heat transfer and fluid dynamic measurements downstream a backward-facing step.
Journal of Heat Transfer 107 (1985), 922–929.